Increases in intracellular calcium perturb blood-brain barrier via protein kinase C-alpha and apoptosis

Kamini Rakkar[a] and Ulvi Bayraktutan[a*]

[a] Stroke, Division of Clinical Neuroscience, Clinical Sciences Building, School of Medicine, Hucknall Road, Nottingham, NG5 1PB, UK

*Corresponding author
Dr Ulvi Bayraktutan,
Associate Professor
Stroke, Division of Clinical Neuroscience
Clinical Sciences Building
School of Medicine
The University of Nottingham
Hucknall Road
Nottingham
NG5 1PB
UK

Tel: +44 1158231764
E-mail: ulvi.bayraktutan@nottingham.ac.uk

Running title

Ca^{2+} damages BBB via PKCα and apoptosis

Abstract

An increase in intracellular calcium represents one of the early events during an ischaemic stroke. It triggers many downstream processes which promote the formation of brain oedema, the leading cause of death after an ischaemic stroke. As impairment of blood-brain barrier (BBB) accounts for much of oedema formation, the current study explored the impact of intracellular calcium on barrier integrity in relation to protein kinase C, caspase-3/7, plasminogen activators and the pro-oxidant enzyme NADPH oxidase. Human brain microvascular endothelial cells alone or in co-culture with human astrocytes were subjected to 4 hours of oxygen-glucose deprivation alone or followed by 20 hours of reperfusion (OGD±R) in the absence or presence of inhibitors for urokinase plasminogen activator (amiloride), NADPH oxidase (apocynin), intracellular calcium (BAPTA-AM) and protein kinase C-α (RO-32-0432). Endothelial cells with protein kinase C-α knockdown, achieved by siRNA, were also exposed to the above conditions. BBB permeability was measured by transendothelial electrical resistance and Evan's blue-albumin and sodium fluorescein flux. Intracellular calcium and total superoxide anion levels, caspase-3/7, NADPH oxidase, plasminogen activator and protein kinase C activities, stress fibre formation, the rate of apoptosis and BBB permeability were increased by OGD±R. Treatment with the specific inhibitors or knockdown of protein kinase C-α attenuated them. This study reveals successive increases in intracellular calcium levels and protein kinase C-α activity are key mechanisms in OGD±R-mediated impairment of BBB. Furthermore inhibition of protein kinase C-α may be therapeutic in restoring BBB function by reducing the rate of cytoskeletal reorganisation, oxidative stress and apoptosis.

Keywords:

Apoptosis; blood-brain barrier; intracellular calcium; NADPH oxidase; protein kinase C; urokinase

Abbreviations

N,N'-[1,2-ethanediylbis(oxy-2,1-phenylene)]bis[N-[2-[(acetyloxy)methoxy]-2-oxoethyl]]-, bis[(acetyloxy)methyl] ester (BAPTA-AM), blood-brain barrier (BBB); bovine serum albumin (BSA); bovine brain microvascular endothelial cells (BBMEC); central nervous system (CNS); Evan's blue albumin (EBA); foetal bovine serum (FBS); Hank's Balanced Salt Solution (HBSS); human astrocytes (HA); human brain microvascular endothelial cells (HBMEC); inositol-1,4,5-triphosphate (IP3); normoxia (N); oxygen-glucose deprivation with/out reperfusion (OGD±R); phosphate buffered saline (PBS); protein kinase C (PKC); phorbol-12-myristate-13-acetate (PMA); reactive oxygen species (ROS); small interfering RNA (siRNA); sodium fluorescein (NaF); superoxide anion ($O_2^{\bullet-}$); tissue plasminogen activator (tPA); transendothelial electrical resistance (TEER); urokinase plasminogen activator (uPA)

1. Introduction

The blood-brain barrier (BBB) is composed of tightly packed endothelial cells surrounded by astrocytic endfeet, a basement membrane, pericytes and neurones. It regulates the passage of circulating molecules into the brain, maintaining central nervous system (CNS) homeostasis. Hence, any pathology capable of affecting BBB integrity would have dramatic consequences for the CNS [1]. During an ischaemic stroke, affected cells experience an intracellular calcium overload due to depletion of ATP and subsequent ion pump dysregulation which result in calcium influx. This increase in intracellular calcium is recognised as one of the first mechanisms that ultimately compromise BBB during an ischaemic stroke. However, the precise molecular targets and cascade of events remain vague. Since calcium is a second messenger and can trigger various signalling pathways depending on its specific localisation within a cell [2, 3] its potential to influence deleterious processes is vast. Furthermore the effect of increasing intracellular calcium can be two-fold; the immediate effect of direct interaction of calcium with proteins and less rapid events which involve changes in gene expression which can be achieved through signal transduction pathways [4].

Calcium overload has also been associated with cell death during ischaemic stroke both via apoptosis and necrosis [5]. The apoptotic pathway can be triggered by many protein cascades and results in caspase-3/7 activation. Many *in vitro* and *in vivo* studies have shown caspases to become activated during ischaemia/reperfusion [6-8] and inhibition of caspases with carbobenzoxy-valyl-alanyl-aspartyl-[O-methyl]-fluoromethylketone has been shown to have beneficial effects in reducing infarct volumes, tight junction disruption and BBB permeability [9-12].

BBB permeability is predominantly governed by the tight junctions between adjacent cells and both low and high levels of calcium have been shown to have an adverse effect on these endothelial cell junctions. Increasing intracellular calcium concentrations has been shown to interfere in tight junction development [13], and lowering calcium levels have been observed to change the cellular localisation of occludin and zonula occluden-actin binding [14]. Furthermore in bovine brain microvascular endothelial cells (BBMEC) exposed to hypoxia-aglycaemia and treated with a calcium channel blocker SKF 96365, occludin cellular localisation and BBB permeability was partially protected [15]. Therefore the ability of endothelial cells to maintain a balance in calcium concentration is vital to their ability to maintain BBB integrity.

Many studies have shown calcium to be a key governor in BBB permeability. In BBMEC cultured with rat astroglioma cells BBB permeability was increased after hypoxia-aglycaemia which was ameliorated by a calcium channel blocker nifedipine indicating the role of calcium flux in BBB permeability [16]. Furthermore in porcine endotheial cells nifedipine also reduced the increase in ischaemia-induced BBB permeability and evidence was provided that blockage of protein kinase C (PKC) translocation to the membrane played a part [17]. In BBMEC intracellular calcium levels were increased after hypoxia/reoxygenation although capacitive calcium entry was inhibited. Furthermore the increase was blocked by superoxide dismutase and inhibitors of mitochondrial electron transport, indicating the role of reactive oxygen species (ROS) in calcium signalling [18].

Calcium regulates many downstream processes such as protein phosphorylation (through PKC) and ROS generation, both of which can regulate protein activity and have been implicated in BBB damage during ischaemic stroke. Conventional (calcium-dependent) PKC isoforms are therefore a key focus in BBB permeability especially since they have been found to be upregulated in hyperglycaemic and ischaemic conditions. In BBMEC, hypoxia/aglycaemia induced expressions of membrane-bound PKC-α and -β_I, [19]. In cultured porcine endothelial cells, ischaemia induced increases in PKC and inhibition of PKC-α reduced endothelial permeability [17] and in rat brain microvessel endothelial cells total PKC activity was increased after hypoxia [20]. PKC is also known to affect cell morphology by activating endothelial contraction [21] which alters adherens and tight junctions and thus evoke BBB permeability [22]. Recent studies have also shown PKC and ROS to be involved in BBB damage under hyperglycaemic conditions. In human brain microvascular endothelial cells (HBMEC) hyperglycaemia induced BBB permeability appeared to be mediated by PKC and subsequent activation of nicotinamide adenine dinucleotide phosphate (NADPH) oxidase activity which elevated total superoxide anion ($O_2^{\bullet-}$) levels and therefore oxidative stress [23, 24]. Similar findings have also been reported in bovine vascular endothelial cells [25].

Another element of BBB hyperpermeability during ischaemic stroke is the increased damage observed during reperfusion which can lead to vasogenic brain oedema. During reperfusion there is a substantial increase in oxidative stress which contributes to BBB impairment [26, 27]. Many studies suggest that increases in ROS levels disrupt endothelial tight junctions, resulting in increased BBB permeability [28-30]. Studies have also shown NADPH oxidase

to be involved in reperfusion injury [31-33] for example in an immortalised Lewis rat cell line, $O_2^{\bullet-}$ has been shown to disrupt tight junctions and induce F-actin polymerisation into stress fibres [34].

Endogenous reperfusion is achieved through the activation of the plasminogen-plasmin system and in particular tissue plasminogen activator (tPA) and urokinase plasminogen activator (uPA). Both these serine proteases cleave plasminogen to form plasmin which then degrades the fibrinous blood clot, restoring blood flow to the occluded vessel and downstream tissue. tPA and uPA have been studied well under ischaemic conditions [35, 36]. The literature however is undecided as to whether these serine proteases are beneficial or damaging [37, 38]. Our previous study has shown both tPA and uPA activities to be upregulated during *in vitro* ischaemia-reperfusion settings and more pertinently to be regulated by ROS [33]. However this area remains largely unexplored and even less well studied, is the link between plasminogen activators and intracellular calcium.

A few studies have shown that tPA can cleave the N-methyl-D-aspartate receptor and induce calcium influx in neurones [39, 40], however studies in endothelial cells are lacking. tPA has also been shown to have both an apoptotic and anti-apoptotic effect on cortical neurones [41, 42]. Studies in human umbilical vein endothelial cells have shown PKC to regulate uPA by upregulating expression of the uPA receptor [43-45]. Some studies have shown the role of uPA in apoptosis in ganglion cells [46] and kidney allograft rejection [47], however studies looking at the BBB are needed.

This study explores the link between calcium-induced signalling cascades such as PKC activation and their role in ROS generation and BBB damage. Additionally this study attempts to take this link further by looking at cell apoptosis, stress fibre formation and plasminogen activator activities under oxygen-glucose deprivation with/out reperfusion (OGD±R).

2. Materials and methods

2.1 Cell culture and OGD±R experiments

HBMEC were purchased from ScienCell and grown to subconfluence in its specialised media (containing 10% FBS) before exposure to OGD (94.5% N_2, 0.5% O_2 and 5% CO_2) or

normoxia (75% N_2, 20% O_2 and 5% CO_2) for 0.5 to 4 hours. These OGD conditions were used to mimic a severe ischaemic attack. In some experiments, OGD was followed by 20 hours of reperfusion in which the RPMI media (ischaemic culture medium lacking glucose, pyruvate and foetal bovine serum (FBS), Sigma) was replaced with fresh HBMEC cell media containing 5.5 mM glucose and 10% FBS before exposing cells to normoxic conditions. In other experiments, amiloride (uPA inhibitor, 2.5 µM, Sigma), apocynin (NADPH oxidase inhibitor, 1 mM, Sigma), BAPTA-AM (intracellular calcium chelator, 10 µM, Merck), bisindolylmaleimide (PKC inhibitor, 5 µM, Calbiochem), LY-333531 (PKC-β inhibitor, 1 µM, Enzo Life Sciences), CGP-53353 (PKC-β_{II} inhibitor, 1 µM, Calbiochem) or RO-32-0432 (PKC-α inhibitor, 1 µM, Calbiochem) was also added to culture media during OGD or reperfusion stages. In other experiments, normoxic HBMEC were exposed to phorbol-12-myristate-13-acetate (PMA, a PKC activator, 0.1 µM, Sigma) with/out BAPTA-AM.

2.2 *In vitro* model of human BBB

Human astrocytes (HA) were purchased from ScienCell and seeded onto the outer surface of untreated polyester Transwell inserts (0.4 µm pore, Corning Costar) seated upside down in HA media. The next day, HBMEC were seeded onto the inner surface of the same inserts in HBMEC media. Both sets of cells were grown to confluence (~5-6 days) in their specialised cell media before exposure and/or treatment. The inserts provided free flow of media and/or any substances produced by the HBMEC and HA to encourage BBB development.

2.3 Assessment of BBB permeability

The BBB integrity and function were studied as previously described [48-51]. Transendothelial electrical resistance (TEER) was measured using STX electrodes and an EVOM resistance meter (World Precision Instruments). To measure Evan's blue-labelled albumin (EBA, 67 kDa) or sodium fluorescein (NaF, 376 Da) flux, inserts were transferred to new 12-well plates containing 2 mL of Hank's Balanced Salt Solution (Sigma). EBA (500 µL, 165 µg/mL, Sigma) or NaF (500 µL, 10 µg/mL, Sigma) was added to the luminal compartments and after 60 minutes samples were taken from both abluminal and luminal chambers. The concentration of dye in each chamber was determined by measuring the absorbance (610 nm, EBA) or fluorescence (excitation 485 nm and emission 520 nm, NaF) of the samples and flux was calculated (abluminal reading x 2000 x luminal reading^{-1}).

2.4 Small interfering RNA (siRNA) knockdown

Subconfluent cells were transfected with ON-TARGET plus SMARTpool human PKC-α (50 nM) or non-targeting (50 nM) siRNA using DharmaFECT transfection reagent 4 (Thermo Scientific) for 16 hours on day one after which the transfection reagent was replaced with HBMEC cell media. On day three the transfection was repeated after which the cells were used in relevant experiments. The sequences of the oligonucleotides used in PKC-α SMARTpool were: UCACUGCUCUAUGGACUUA, GAAGGGUUCUCGUAUGUCA, UUAUAGGGAUCUGAAGUUA and UAAGGAACCACAAGCAGUA.

2.5 Intracellular calcium determination

Intracellular calcium levels were determined using the Fluo-4 NW Calcium Assay kit (Invitrogen). Briefly, cells grown in opaque black 96 well plates (Nunc) were incubated with dye loading solution for 45 minutes to load cells with Fluo-4 AM, an indicator for intracellular calcium. This solution was then removed, the cells washed once with phosphate buffered saline (PBS, Sigma) and then either RPMI or HBMEC media was added to the wells. Cells were then exposed/treated after which the fluorescence was measured (excitation 485 nm and emission 520 nm, room temperature) and buffer blanks subtracted.

2.6 Caspase-3/7 activity

Caspase-3/7 activity was determined using the Apo-ONE Homogenous Caspase-3/7 Assay (Promega) as previously documented [52]. Briefly, cells grown in opaque black 96 well plates were exposed or treated as above after which 100 µL of Apo-ONE Caspase-3/7 reagent was added to each well and the plates frozen immediately at -80°C. After one freeze thaw cycle the fluorescence was measured (excitation 485 nm and emission 520 nm) and buffer blanks subtracted.

2.7 TUNEL staining

To view apoptotic nuclei a DeadEnd Colorimetric TUNEL System was used (Promega). Briefly, HBMEC were grown on coverslips, exposed/treated as above and then fixed with 4% paraformaldehyde (Sigma) in PBS. To enable end-labelling of DNA fragments, coverslips were incubated with a recombinant terminal deoxynucleotidyl transferase reaction mix for 60 minutes at 37°C. Incorporated biotinylated nucleotides were detected by horseradish peroxidase-labelled streptavidin and the chromogen diaminobenzidine which stains apoptotic nuclei dark brown. HBMEC were viewed with a light microscope and average % rate of

apoptosis calculated from 3 different fields per coverslip for one independent experiment from the following equation: (number of apoptotic nuclei / total number of nuclei) x 100.

2.8 PKC activity

PKC activity was determined as before using the PepTag Assay for Non-Radioactive Detection of Protein kinase C (Promega) [53]. Briefly, cell pellets were sonicated in PKC extraction buffer (containing 0.05% Triton X-100) to obtain cytosolic and membranal PKC proteins. The sonicate was passed through a diethylaminoethyl cellulose column. PKC samples were incubated with PepTag C1 peptide, a fluorescent substrate, in a PKC reaction mix (containing calcium and phoshatidylserine) for 30 minutes at 30°C. The PKC reaction mix ensured all components required for PKC activation were present. Samples, including positive (purified active rat PKC) and negative (ultra-pure water) controls, were electrophoresed on a 0.8% agarose gel at 80 V for 45 minutes and the bands visualised under UV light. Bands were excised and their absorbance measured at 570 nm.

For the specific activities of PKC-α and PKC-β_I, the isoforms were immunoprecipitated using respective primary antibodies (Santa Cruz Biotechnology) and Dynabeads protein G (Invitrogen) before using the above assay kit.

2.9 tPA and uPA ELISA

uPA and tPA activities were measured using an ELISA-based assay as previously described [33]. Briefly, 96 well plates were coated with PAI-1 (300 ng/mL; Abcam) to detect and bind active tPA or uPA. Plates were then blocked with 3% bovine serum albumin (BSA, Thermo Fischer Scientific). Equal volumes of cell culture media or uPA and tPA standards (Calbiochem) were added to the PAI-1-coated wells and the plates incubated for 2 hours at room temperature. PAI-1-bound active uPA or tPA was detected by anti-tPA or anti-uPA primary antibodies (1:50, Santa Cruz Biotechnology) and primary antibodies were probed with horseradish peroxidase-linked secondary antibodies (1:5000, Santa Cruz). A colourimetric horseradish peroxidase substrate, 3,3',5,5'-tetramethylbenzidine (Thermo Scientific), was added to the wells to visualise and quantitate PAI-1-tPA/uPA-antibody complexes. The reaction was stopped with H_2SO_4 and absorbances were read immediately at 450 nm and normalised against the respective standards and total protein concentrations.

2.10 Total $O_2^{\bullet-}$ production and NADPH oxidase activity

Total $O_2^{\bullet-}$ levels were determined using the cytochrome *C* reduction assay [48]. Briefly, cell pellets were sonicated in cold lysis buffer containing HEPES buffer (20 mM, pH 7.2, Calbiochem), ethylene glycol tetraacetic acid (1 mM, Sigma), mannitol (210 mM, Sigma) and sucrose (70 mM, Sigma). Equal amounts of homogenate (100 µg) were incubated with cytochrome *C* (50 µM, Sigma) at 37°C for 60 minutes before absorbances were measured at 550 nm.

NADPH oxidase activity was measured with the lucigenin chemiluminescence assay [51]. Briefly, samples of homogenates (~100 µg) were processed as above then incubated at 37°C in assay buffer containing potassium phosphate buffer (50 mM, pH 7.0, Sigma), ethylene glycol tetraacetic acid (1 mM), sucrose (150 mM) and lucigenin (5 µM, Sigma). The assay buffer also contained the specific inhibitors for other ROS-generating enzymes; nitric oxide synthase (NG-nitro-L-arginine methyl ester, 100 µM, Sigma), mitochondrial complex I (rotenone, 50 µM, Sigma), xanthine oxidase (allopurinol, 100 µM, Sigma) and cyclooxygenase (indomethacin, 50 µM, Sigma). After 15 minutes, NADPH (100 µM; Calbiochem) was added to initiate the reaction. The reaction was monitored every minute for 2 hours and the rate of reaction calculated. Buffer blanks were also run for both assays and subtracted from the data.

2.11 Western blotting

HBMEC were harvested with 0.1% Triton X-100 (Sigma) in PBS containing 1 mg/ml aprotinin, 10 mg/ml leupeptin and 1 mM phenylmethylsulfonyl fluoride. The lysate was centrifuged at 11500 x g for 20 minutes at 4°C. Protein concentration was quantified using the Bradford Protein Assay Kit (Pierce). Protein samples (50 µg) were run on a 10% SDS-polyacrylamide gels before transferring onto Hybond-P PVDF membrane (GE healthcare). Membranes were blocked with 5% milk then exposed to PKC-α (1:500, Santa Cruz Biotechnology) and β-actin (1:15,000, Sigma) primary antibodies followed by infrared dye-tagged secondary antibodies (1:30,000, LI-COR Biosciences). The bands were detected and analysed using the Odyssey Infrared Imaging System.

2.12 F-actin staining

HBMEC grown on coverslips to ~80% confluence were exposed to experimental conditions before successively fixing, permeabilising and blocking with 4% paraformaldehyde, 0.1%

Triton X-100 and 1% BSA for 20 minutes each. Cells were stained in the dark with rhodamine phalloidin dye (20 U/mL, Invitrogen) for 20 minutes then washed with PBS. Finally cells were stained with DAPI (1 ug/mL) and visualised with fluorescence microscopy.

2.13 Cell viability

An aliquot of cells were mixed with 0.1% Trypan blue and visualised under a light microscope. Percentage viability was calculated from counting 100 cells.

2.14 Statistical analyses

Data are presented as mean±SEM from at least 3 independent experiments. Statistical analyses were performed using one way ANOVA followed by a Tukey post hoc analysis or, where appropriate, by an independent Student's *t*-test. $p<0.05$ was considered as significant.

3. Results

3.1 OGD±R increase intracellular calcium levels, caspase-3/7 activity and apoptosis

Exposure of HBMEC to OGD (0.5-4 hrs) alone or followed by 20 hours of reperfusion led to significant increases in intracellular calcium levels, caspase-3/7 activity (Fig. 1A-B) and apoptosis rate as ascertained by TUNEL staining (Fig. 2A-B), as early as 30 minutes of OGD. Interestingly, while reperfusion augmented the increases observed in calcium levels, it decreased those seen in caspase-3/7 activity and apoptosis rates. As the impact of 4 hrs of OGD±R on the above parameters was slightly higher, albeit not significantly so, this time period was chosen for all subsequent experiments. It is noteworthy that this time point is clinically relevant [54] and consistent with previous studies [33].

3.2 PKC activity is increased during OGD±R

To determine the specific conventional PKC isoform(s) that are affected by ischaemic injury, HBMEC were exposed to OGD±R in the absence or presence of specific inhibitors for PKC-α (RO-32-0432) [55], -β (LY-333531) [56] and -β_{II} (CGP-53353) [57]. OGD±R evoked a significant increase in PKC activity which were normalised by inhibition of total PKC activity with bisindolylmaleimide [58] (Fig. 3A). HBMEC treated with RO-32-0432 showed equally suppressed PKC activity in both OGD and reperfusion stages compared to untreated

cells. Treatment with LY-333531 and CGP-53353 also showed significant decreases in PKC activity compared to untreated cells however higher levels of activity were observed during the reperfusion stage compared to OGD alone (Fig. 3B). To probe PKC-α and -β_I activities directly, the isoforms were immunoprecipitated before performing the PKC activity assay. The activities of both isoforms were significantly increased during OGD±R compared to normoxic cells (Fig. 3C-D). Since the use of RO-32-0432 produced similar levels of total PKC inhibition during both OGD and reperfusion it would appear that PKC-α activity is the most consistent during OGD±R and therefore this isoform was studied further in the experiments below.

3.3 BAPTA-AM attenuates the rise in PKC activity during OGD±R

As conventional PKC isoforms require calcium for their activity [59], reduction of intracellular calcium in HBMEC with BAPTA-AM [60] expectedly decreased the OGD±R-mediated rise in PKC activity (Fig. 3E). To test whether BAPTA-AM had a direct effect on PKC activity, PMA, a proven PKC activator [61], was used to induce PKC activity. As expected, PMA significantly enhanced PKC activity which was normalised by co-exposure or pre-exposure (4 h) with BAPTA-AM (Fig. 3F). PMA also markedly increased PKC-α activity (Fig. 3G).

3.4 Inhibition of uPA and NADPH oxidase attenuates OGD±R-evoked increases in PKC-α activity

Inhibition of uPA and NADPH oxidase in HBMEC exposed to OGD±R normalised the stimulatory effects of both phenomena on total PKC and PKC-α activities (Fig. 4A-B). However since the uPA inhibitor, amiloride, has known effects of inhibiting Na+ and Na+/H+ exchange channels it is possible these effects may also be due to inhibition of these channels as well as uPA. To determine the effect of intracellular calcium and PKC-α on plasminogen activators, the activities of tPA and uPA were determined in cells subjected to OGD±R with BAPTA-AM or RO-32-0432. Similar to a previous study while OGD±R induced tPA and uPA activities [33], chelation of intracellular calcium or inhibition of PKC-α selectively reduced uPA activity albeit remaining slightly but insignificantly higher compared to normoxic cells with the RO-32-0432 treatment (Fig. 4C-D).

3.5 Inhibition of PKC-α reduces total $O_2^{\bullet-}$ levels and NADPH oxidase activity

To test whether $O_2^{\bullet-}$ or NADPH oxidase activity is affected by intracellular calcium, total PKC and PKC-α, HBMEC were exposed to OGD±R with or without BAPTA-AM, bisindolylmaleimide or RO-32-0432. In support of our recent study [33], reperfusion has been shown to further potentiate the increases observed in total $O_2^{\bullet-}$ and NADPH oxidase activity evoked by OGD. Although all the aforementioned inhibitors reduced both increases (Fig. 5A-D), the levels still remained significantly higher than normoxic cells with bisindolylmaleimide and RO-32-0432 treatment. To examine the direct effect of PKC activity, HBMEC were exposed to PMA which significantly increased both total $O_2^{\bullet-}$ levels and NADPH activity where addition of BAPTA-AM reversed these increases (Fig. 5E-F).

3.6 Rises in calcium levels and caspase-3/7 activity are attenuated by amiloride, apocynin, BAPTA-AM and RO-32-0432

HBMEC were exposed to OGD±R and treated with amiloride, apocynin, BAPTA-AM or RO-32-0432. Amiloride and apocynin significantly reduced increases in intracellular calcium levels during reperfusion only whereas BAPTA-AM reduced calcium levels during OGD and reperfusion. However since amiloride can also inhibit Na+ channels and the Na+/H+ exchanger, it is possible that the above effects are not entirely due to uPA inhibition. RO-32-0432 significantly reduced calcium levels during both OGD and reperfusion although levels remain elevated compared to normoxic cells (Fig. 6A). All the inhibitors mentioned also significantly reduced the increases observed in caspase-3/7 activity during OGD and reperfusion however activity levels in cells treated with apocynin and amiloride still remained higher than normoxic cells during reperfusion (Fig. 6B).

3.7 PKC-α silencing reduces OGD±R-evoked increases in calcium levels, caspase-3/7 activity and apoptosis rate

To look directly at PKC-α activity and establish results with RO-32-0432, PKC-α gene expression was silenced using specific siRNA. PKC-α knockdown significantly reduced PKC-α protein levels compared to control cells and cells exposed to non-targeting siRNA (Fig. 7). PKC-α knockdown significantly reduced caspase-3/7 activity and the rate of apoptosis compared to cells exposed to OGD±R, however the rate remained significantly higher than normoxic cells. TUNEL staining also showed fewer apoptotic nuclei with PKC-α siRNA compared to NT siRNA (Fig. 8A-B).

3.8 Amiloride, apocynin, BAPTA-AM and RO-32-0432 reduced the rate of apoptosis during OGD±R

To examine the specific relevance of uPA, NADPH oxidase, intracellular calcium and PKC-α to cell viability, HBMEC were exposed to OGD±R in the presence of their respective inhibitors before viewing apoptotic nuclei via a TUNEL kit. All inhibitors dramatically reduced the rate of OGD±R-mediated apoptosis however the rate remained significantly elevated compared to normoxic cells (Fig. 9).

3.9 OGD±R induces stress fibre formation

HBMEC grown on coverslips were exposed to OGD±R in the absence or presence of aforementioned enzyme inhibitors. Cells targeted with PKC-α siRNA or non-targeting siRNA were also exposed to OGD±R. All the above inhibitors and PKC-α siRNA showed reduced or no stress fibre formation when compared to HBMEC exposed to OGD±R alone (Fig. 10).

3.10 Suppression of PKC-α activity protects the BBB during OGD±R

Ultimately the usefulness of PKC-α inhibition was determined on a co-culture model of the BBB comprised of HBMEC and HA. OGD±R significantly increased BBB permeability as observed by decreases in TEER and increases in EBA and NaF flux. Furthermore, reperfusion showed significantly lower TEER values and higher flux volumes compared to OGD alone, supporting previous data [33]. Chelation of intracellular calcium normalised TEER values and EBA flux volumes where NaF volumes remained significantly higher than normoxic cells (Fig. 11A-C). PKC-α suppression via siRNA also restored BBB permeability as indicated by significant increases in TEER values and reductions in flux volumes compared to untreated cells (Fig. 11D-F). To determine the effect of BAPTA-AM and PKC-α siRNA on PKC activity co-cultures were exposed to PMA before treatment. PMA increased BBB damage which was reversed with BAPTA-AM or PKC-α knockdown. Double treatment with both BAPTA-AM and PKC-α siRNA showed a slight benefit over single treatment as observed by completely normalised TEER values and paracellular flux (Fig. 11G-I).

4. Discussion

Interruption of blood flow during an ischaemic stroke results in a cascade of molecular events which elicit BBB damage and may be exacerbated during reperfusion [62]. An increase in intracellular calcium is one of the first events which trigger these harmful cellular cascades and our study shows intracellular calcium to not only be increased as early as 30 minutes of OGD but to still be elevated at 20 hours of reperfusion [63, 64].

Calcium has been a therapeutic target in ischaemic stroke and calcium channel blockers have been shown to have therapeutic relevance in neurones such as nimodipine, an L-type channel blocker which has been shown to improve cerebral blood flow and metabolic rates in humans [65, 66]. However not much is known about the role of calcium in BBB damage. Indeed, there is no firm proof that clinical outcome after stroke is improved with calcium channel blockers [67, 68]. The present study suggests that chelation of intracellular calcium is an effective therapeutic option in HBMEC and *in vitro* BBB damage.

As the presence of astrocytes is a prerequisite for appropriate expression and localisation of endothelial cell tight junction proteins, a HBMEC-HA contact co-culture model was employed throughout this study to measure BBB permeability [69, 70]. Although the normoxic barrier function may be considerably lower than *in vivo* studies, the contact co-culture model employed in this study has been shown to be one of the most reliable *in vitro* models of human BBB in previous studies [24, 48]. Indeed, similar to *in vivo* settings, the close proximity ($\leq$10 μM) between endothelial cell and astrocyte layers in this model allows cells to effectively communicate with one another and respond to agents that may be released by the other cell line. This feature of the contact co-culture model was of particular importance in discovering presence of endothelial cells as an important prerequisite for maintaining higher rates of astrocytic viability as ascertained by lower apoptosis rates of astrocytes cultured in endothelial cell conditioned medium [52].

It is possible that the varying results obtained with calcium antagonists may be due to their different specificities for different types of neuronal calcium channels [71] and the different treatment times, where pre-dosing of the animals was seen to be most effective [72]. More importantly, these antagonists block extracellular calcium from entering and increasing intracellular calcium levels. Therefore it is likely that calcium released from intracellular sources such as the endoplasmic reticulum and mitochondria can sufficiently increase intracellular calcium levels under stress [73] and affect various downstream signalling

pathways such as PKC [74]. Therefore the buffering of intracellular calcium ions may prove to be more effective as shown in the current study.

Our results show that conventional PKC isoforms are predominantly activated during OGD±R, similar to findings in other pathologies such as hyperglycaemia [23, 24], with PKC-α inhibition and gene silencing shown to be an important therapeutic intervention. Additionally chelation of intracellular calcium proved to be a pivotal inhibitory mechanism for PKC, substantiating its role as an initiator of this deleterious cascade. Indeed, it has been shown that the use of BAPTA, a non-cell permeable chelator of calcium, did not affect increases in PKC activity [61] further supporting the hypothesis that cytosolic calcium triggers signalling cascades detrimental to BBB permeability.

Investigating these findings deeper, inhibition of PKC-α with RO-32-0432 was shown to downregulate OGD±R-induced uPA activity whereas calcium-chelation completely normalised it. These results not only suggest the involvement of other calcium-dependent PKC isoforms in uPA regulation but also prove the effective inhibition of PKC with BAPTA-AM. Given that BAPTA-AM is an intracellular calcium chelator, its inhibitory effects on uPA activity are likely to be more diverse than the sole inhibition of PKC and to include inhibition or downregulation of other calcium-dependent cascades. Conversely inhibition of PKC-α and chelation of intracellular calcium did not affect tPA activity. Therefore it is possible that tPA may operate upstream to these mechanisms.

The OGD±R-mediated increases observed in both plasminogen activator activities were consistent with the present literature [38, 75]. Inhibition of uPA by amiloride [76] downregulated both total PKC and PKC-α activities and thus implied a reciprocal relationship between uPA and PKC. However since amiloride is known to inhibit Na^+/H^+ exchange and Na^+ channels generally at higher concentrations (>130 μM), it is possible the effects seen from its use may also be due to inhibition of these channels. Amiloride has been observed to be a specific inhibitor for uPA at lower concentrations such as that used in the current study [76] however its implications in ion channel inhibition cannot be discounted therefore interpretation of the data needs to be done with caution.

The regulation of uPA activity by PKC is well-documented [43-45] however the reverse is much less explored. Interaction of uPA with its receptor may indirectly affect PKC activity via mitogen-activated protein kinases which despite regulating both uPA and PKC separately

may also be able to connect them [77-79]. Moreover, impairment of glucose uptake has also shown uPA to indirectly affect PKC activity [80] which may be a prominent factor in OGD studies.

The use of amiloride selectively attenuated rises in intracellular calcium during reperfusion but not OGD, an effect mimicked by inhibition of NADPH oxidase. This difference between the two stages is somewhat surprising. Lack of glucose and associated ATP production and therefore failure of ion pumps and influx of calcium may explain ineffectiveness of uPA and NADPH oxidase suppression in affecting calcium levels during OGD phase [62] whereas during reperfusion when ATP production is re-established and therefore ion pumps are working the inhibition of uPA and NADPH oxidase may be more apparent.

The relationship between calcium and uPA or NADPH oxidase remains largely unknown. uPA binding to its receptor has been shown to increase intracellular calcium concentrations in phagocytes [81] and stimulate production of inositol-1,4,5-triphosphate (IP3) which then releases calcium from intracellular stores [82]. In skeletal muscle, NADPH oxidase activation was required for intracellular calcium increases [81-86] and in human endothelial cells, NADPH oxidase increased calcium release via IP3 [84, 85].

Conversely, other studies have shown that vascular cell adhesion molecule-1-induced calcium mobilisation is required for NADPH oxidase activity in lymphocytes [87] and that calcium is required for activation of Nox5, a NADPH oxidase isoform [86]. Similar to studies with amlodipine, a calcium channel blocker, which reduced NADPH oxidase activity [88] and oxidative stress [89] in rats, our study showed calcium chelation completely normalised $O_2^{\bullet-}$ levels and NADPH oxidase activity. Our study further suggests this is in part mediated through PKC since PKC inhibition was shown to also reduce oxidative stress albeit to a lesser extent indicating that other calcium-dependent mechanisms also contribute to oxidative stress and PKC activation is not the only mechanism that induces NADPH oxidase activity and $O_2^{\bullet-}$ production. Indeed other pathologies arising from ischaemia-reperfusion injury including the excessive release of pro-inflammatory cytokine tumour necrosis factor-α [52] and ROS due to increased mitochondrial calcium levels [90] can contribute to oxidative stress.

Our results also suggest that NADPH oxidase and PKC reciprocally activate each other. This may partly be due to the sensitivity of PKC for oxidants like $O_2^{\bullet-}$ which can modify its N-terminal regulatory domains making it more resistant to autoinhibition [91] and also through

phosphorylation of NADPH oxidase subunits by PKC which increases the overall activity of the oxidase complex [92, 93].

The results from this study indicate that abolishing the activity of one enzymatic target alone is not enough to completely reverse cell death and that combination therapy may be required. It would appear that some cell death is inevitable and future experiments looking at combination therapy and far reaching targets of the enzymes involved are needed. For example, some studies suggest matrix metalloproteinase-2 and -9 may induce caspase-3 activation [94] and since our previous study has linked matrix metalloproteinase-2 to uPA and NADPH oxidase activity [33], it is possible that in HBMEC caspase-3/7 activation is also mediated by matrix metalloproteinase-2. Additionally in our previous study [33] uPA was shown to operate upstream to NADPH oxidase and this study now indicates the involvement of PKC in this relationship.

All the above inhibitors also markedly decreased OGD±R-evoked actin polymerisation, revealing that all the components discussed have a role in cytoskeletal infrastructure which is necessary for maintenance of cell morphology and function. Pathologies capable of affecting actin redistribution and polymerisation to form stress fibres have been shown to increase tight junctional permeability [52, 95-97]. Also in rat brain microvascular endothelial cells exposure to OGD±R induced ROS formation, caspase-3 activity, stress fibre formation and tight junction disruption and inhibition of ROS and caspase-3 attenuated BBB hyperpermeability through protection of tight junctions and the cytoskeleton [98].

Prevention of BBB damage during or restoration of the BBB after an ischaemic stroke is a priority and any potential therapeutic targets need to be assessed against their ability to do this. Inhibition of uPA and NADPH oxidase has been shown in a previous study to restore BBB integrity [33] and in the present study chelation of intracellular calcium and knockdown of PKC-α has also shown this effect. Indeed even in the presence of PMA, BAPTA-AM and PKC-α siRNA have been shown to have a beneficial effect indicating the major role played by intracellular calcium and PKC-α.

5. Conclusions

This study shows that in HBMEC exposed to OGD±R many individual events occur which ultimately compromise BBB function. Furthermore these events appear to be interlinked in a complex manner. This study strongly suggests intracellular calcium is a key mediator of BBB damage during OGD±R and the mechanism of increased BBB permeability is an increase in HBMEC apoptosis mediated through a reciprocal PKC-uPA-NADPH oxidase pathway which warrants exploring in greater detail for possible therapeutic outcomes. Furthermore although many studies conducted with calcium channel blockers show neuroprotection, the results with regards to stroke outcome are inconclusive partly due to hypotensive effect of these drugs and associated complications. Therefore studies examining BBB function and intracellular calcium levels regardless of the source are needed to define the calcium-induced mechanism of BBB disruption. Therapeutic interventions which target buffering of intracellular calcium without affecting blood pressure are a possible avenue of exploration.

6. Acknowledgements

This study was funded by a Medical Research Council Doctoral Training Grant to Dr Bayraktutan.

7. References

[1] K. Hayashi, S. Nakao, R. Nakaoke, S. Nakagawa, N. Kitagawa, M. Niwa, Effects of hypoxia on endothelial/pericytic co-culture model of the blood-brain barrier, Regul. Pept., 123 (2004) 77-83.
[2] D.D. Ginty, Calcium regulation of gene expression: Isn't that spatial?, Neuron, 18 (1997) 183-186.
[3] F.H. Cruzalegui, H. Bading, Calcium-regulated protein kinase cascades and their transcription factor targets, Cell. Mol. Life Sci., 57 (2000) 402-410.
[4] K.A. Seta, Y. Yuan, Z. Spicer, G. Lu, J. Bedard, T.K. Ferguson, P. Pathrose, A. Cole-Strauss, A. Kaufhold, D.E. Millhorn, The role of calcium in hypoxia-induced signal transduction and gene expression, Cell Calcium, 36 (2004) 331-340.
[5] S. Mitra, R. Gera, W.A. Siddiqui, S. Khandelwal, Tributyltin induces oxidative damage, inflammation and apoptosis via disturbance in blood-brain barrier and metal homeostasis in cerebral cortex of rat brain: An in vivo and in vitro study, Toxicology, 310 (2013) 39-52.
[6] X. Wang, B.E. Figueroa, I.G. Stavrovskaya, Y. Zhang, A.C. Sirianni, S. Zhu, A.L. Day, B.S. Kristal, R.M. Friedlander, Methazolamide and Melatonin Inhibit Mitochondrial Cytochrome C Release and Are Neuroprotective in Experimental Models of Ischemic Injury, Stroke, 40 (2009) 1877-1885.

[7] H.-C. Pan, T.-K. Kao, Y.-C. Ou, D.-Y. Yang, Y.-J. Yen, C.-C. Wang, Y.-H. Chuang, S.-L. Liao, S.-L. Raung, C.-W. Wu, A.-N. Chiang, C.-J. Chen, Protective effect of docosahexaenoic acid against brain injury in ischemic rats, Journal of Nutritional Biochemistry, 20 (2009) 715-725.
[8] D. Jia, B. Han, S. Yang, J. Zhao, Anemonin Alleviates Nerve Injury After Cerebral Ischemia and Reperfusion (I/R) in Rats by Improving Antioxidant Activities and Inhibiting Apoptosis Pathway, J. Mol. Neurosci., 53 (2014) 271-279.
[9] C. Wiessner, D. Sauer, D. Alaimo, P.R. Allegrini, Protective effect of a caspase inhibitor in models for cerebral ischemia in vitro and in vivo, Cell. Mol. Biol., 46 (2000) 53-62.
[10] S.R. Lee, E.H. Lo, Interactions between p38 mitogen-activated protein kinase and caspase-3 in cerebral endothelial cell death after hypoxia-reoxygenation, Stroke, 34 (2003) 2704-2709.
[11] C.M. Zehendner, L. Librizzi, M. de Curtis, C.R.W. Kuhlmann, H.J. Luhmann, Caspase-3 Contributes to ZO-1 and Cl-5 Tight-Junction Disruption in Rapid Anoxic Neurovascular Unit Damage, PLoS One, 6 (2011).
[12] S. Park, M. Yamaguchi, C. Zhou, J.W. Calvert, J. Tang, J.H. Zhang, Neurovascular protection reduces early brain injury after subarachnoid hemorrhage, Stroke, 35 (2004) 2412-2417.
[13] R.O. Stuart, A. Sun, K.T. Bush, S.K. Nigam, Dependence of epithelial intercellular junction biogenesis on thapsigargin-sensitive intracellular calcium stores, J. Biol. Chem., 271 (1996) 13636-13641.
[14] J.M. Ye, T. Tsukamoto, A. Sun, S.K. Nigam, A role for intracellular calcium in tight junction reassembly after ATP depletion-repletion, American Journal of Physiology-Renal Physiology, 277 (1999) F524-F532.
[15] R.C. Brown, T.P. Davis, Hypoxia/aglycemia alters expression of occludin and actin in brain endothelial cells, Biochem. Biophys. Res. Commun., 327 (2005) 1114-1123.
[16] T.J. Abbruscato, T.P. Davis, Combination of hypoxia/aglycemia compromises in vitro blood-brain barrier integrity, J. Pharmacol. Exp. Ther., 289 (1999) 668-675.
[17] A. Hempel, C. Lindschau, C. Maasch, M. Mahn, R. Bychkov, T. Noll, F.C. Luft, H. Haller, Calcium antagonists ameliorate ischemia-induced endothelial cell permeability by inhibiting protein kinase C, Circulation, 99 (1999) 2523-2529.
[18] C. Kimura, M. Oike, Y. Ito, Hypoxia-induced alterations in Ca2+ mobilization in brain microvascular endothelial cells, American Journal of Physiology-Heart and Circulatory Physiology, 279 (2000) H2310-H2318.
[19] T.Z. Yang, K.E. Roder, G.J. Bhat, T.J. Thekkumkara, T.J. Abbruscato, Protein kinase C family members as a target for regulation of blood-brain barrier Na,K,2Cl-cotransporter during in vitro stroke conditions and nicotine exposure, Pharm. Res., 23 (2006) 291-302.
[20] M.A. Fleegal, S. Hom, L.K. Borg, T.P. Davis, Activation of PKC modulates blood-brain barrier endothelial cell permeability changes induced by hypoxia and posthypoxic reoxygenation, American Journal of Physiology-Heart and Circulatory Physiology, 289 (2005) H2012-H2019.
[21] J.G.N. Garcia, H.W. Davis, C.E. Patterson, Regulation of endothelial-cell gap formation and barrier dysfunction - role of myosin light-chain phosphorylation, J. Cell. Physiol., 163 (1995) 510-522.
[22] C. Tiruppathi, R.D. Minshall, B.C. Paria, S.M. Vogel, A.B. Malik, Role of Ca2+ signaling in the regulation of endothelial permeability, Vascul. Pharmacol., 39 (2002) 173-185.
[23] B. Shao, U. Bayraktutan, Hyperglycaemia promotes human brain microvascular endothelial cell apoptosis via induction of protein kinase C-SSI and prooxidant enzyme NADPH oxidase, Redox Biol, 2 (2014) 694-701.

[24] B. Shao, U. Bayraktutan, Hyperglycaemia promotes cerebral barrier dysfunction through activation of protein kinase C-beta, Diabetes Obesity & Metabolism, 15 (2013) 993-999.
[25] T. Inoguchi, P. Li, F. Umeda, H.Y. Yu, M. Kakimoto, M. Imamura, T. Aoki, T. Etoh, T. Hashimoto, M. Naruse, H. Sano, H. Utsumi, H. Nawata, High glucose level and free fatty acid stimulate reactive oxygen species production through protein kinase C-dependent activation of NAD(P)H oxidase in cultured vascular cells, Diabetes, 49 (2000) 1939-1945.
[26] J.H. Heo, S.W. Han, S.K. Lee, Free radicals as triggers of brain edema formation after stroke, Free Radic. Biol. Med., 39 (2005) 51-70.
[27] P. Lagrange, I.A. Romero, A. Minn, P.A. Revest, Transendothelial permeability changes induced by free radicals in an in vitro model of the blood-brain barrier, Free radical biology & medicine, 27 (1999) 667-672.
[28] R.K. Rao, S. Basuroy, V.U. Rao, K.J. Karnaky, A. Gupta, Tyrosine phosphorylation and dissociation of occludin-ZO-1 and E-cadherin-beta-catenin complexes from the cytoskeleton by oxidative stress, Biochem. J., 368 (2002) 471-481.
[29] G. Schreibelt, G. Kooij, A. Reijerkerk, R. van Doorn, S.I. Gringhuis, S. van der Pol, B.B. Weksler, I.A. Romero, P.O. Couraud, J. Piontek, I.E. Blasig, C.D. Dijkstra, E. Ronken, H.E. de Vries, Reactive oxygen species alter brain endothelial tight junction dynamics via RhoA, PI3 kinase, and PKB signaling, FASEB J., 21 (2007) 3666-3676.
[30] P. Sheth, S. Basuroy, C.Y. Li, A.P. Naren, R.K. Rao, Role of phosphatidylinositol 3-kinase in oxidative stress-induced disruption of tight junctions, J. Biol. Chem., 278 (2003) 49239-49245.
[31] H. Hong, J.S. Zeng, D.L. Kreulen, D.I. Kaufman, A.F. Chen, Atorvastatin protects against cerebral infarction via inhibition of NADPH oxidase-derived superoxide in ischemic stroke, American journal of physiology. Heart and circulatory physiology, 291 (2006) H2210-2215.
[32] H.K. Eltzschig, C.D. Collard, Vascular ischaemia and reperfusion injury, British medical bulletin, 70 (2004) 71-86.
[33] K. Rakkar, K. Srivastava, U. Bayraktutan, Attenuation of urokinase activity during experimental ischaemia protects the cerebral barrier from damage through regulation of matrix metalloproteinase-2 and NAD(P)H oxidase, Eur. J. Neurosci., 39 (2014) 2119-2128.
[34] A. van der Goes, D. Wouters, S.M.A. van der Pol, R. Huizinga, E. Ronken, P. Adamson, J. Greenwood, C.D. Dijkstra, H.E. de Vries, Reactive oxygen species enhance the migration of monocytes across the blood-brain barrier in vitro, FASEB J., 15 (2001) 1852-+.
[35] G.A. Rosenberg, M. Navratil, F. Barone, G. Feuerstein, Proteolytic cascade enzymes increase in focal cerebral ischemia in rat, J. Cereb. Blood Flow Metab., 16 (1996) 360-366.
[36] M. Yepes, M. Sandkvist, E.G. Moore, T.H. Bugge, D.K. Strickland, D.A. Lawrence, Tissue-type plasminogen activator induces opening of the blood-brain barrier via the LDL receptor-related protein, J. Clin. Invest., 112 (2003) 1533-1540.
[37] E. Cho, K.J. Lee, J.W. Seo, C.J. Byun, S.J. Chung, D.C. Suh, P. Carmeliet, J.Y. Koh, J.S. Kim, J.Y. Lee, Neuroprotection by urokinase plasminogen activator in the hippocampus, Neurobiology of disease, 46 (2012) 215-224.
[38] N. Hosomi, J. Lucero, J.H. Heo, J.A. Koziol, B.R. Copeland, G.J. del Zoppo, Rapid differential endogenous plasminogen activator expression after acute middle cerebral artery occlusion, Stroke, 32 (2001) 1341-1348.
[39] A.L. Samson, S.T. Nevin, D. Croucher, B.e. Niego, P.B. Daniel, T.W. Weiss, E. Moreno, D. Monard, D.A. Lawrence, R.L. Medcalf, Tissue-type plasminogen activator requires a co-receptor to enhance NMDA receptor function, J. Neurochem., 107 (2008) 1091-1101.
[40] J. Kaur, Z.G. Zhao, G.M. Klein, E.H. Lo, A.M. Buchan, The neurotoxicity of tissue plasminogen activator?, J. Cereb. Blood Flow Metab., 24 (2004) 945-963.

[41] G. Liot, B.D. Roussel, N. Lebeurrier, K. Benchenane, J.P. Lopez-Atalaya, D. Vivien, C. Ali, Tissue-type plasminogen activator rescues neurones from serum deprivation-induced apoptosis through a mechanism independent of its proteolytic activity, J. Neurochem., 98 (2006) 1458-1464.
[42] O. Nicole, F. Docagne, C. Ali, I. Margaill, P. Carmeliet, E.T. MacKenzie, D. Vivien, A. Buisson, The proteolytic activity of tissue-plasminogen activator enhances NMDA receptor-mediated signaling, Nat. Med., 7 (2001) 59-64.
[43] H. Matsumoto, S. Ueshima, H. Fukao, Y. Mitsui, O. Matsuo, Identification of urokinase-type plasminogen activator receptor in human endothelial cells and its modulation by phorbol myristate acetate, Cell Struct. Funct., 20 (1995) 429-437.
[44] T. Chavakis, A.K. Willuweit, F. Lupu, K.T. Preissner, S.M. Kanse, Release of soluble urokinase receptor from vascular cells, Thromb. Haemost., 86 (2001) 686-693.
[45] D.J. Langer, A. Kuo, K. Kariko, M. Ahuja, B.D. Klugherz, K.M. Ivanics, J.A. Hoxie, W.V. Williams, B.T. Liang, D.B. Cines, E.S. Barnathan, Regulation of the endothelial-cell urokinase-type plasminogen-activator receptor - evidence for cyclic-AMP dependent and protein-kinase-C dependent pathways, Circ. Res., 72 (1993) 330-340.
[46] X. Zhang, A. Chaudhry, S. Chintala, Inhibition of plasminogen activation protects against ganglion cell loss in a mouse model of retinal damage, Mol. Vis., 9 (2003) 238-248.
[47] F. Gueler, S. Rong, M. Mengel, J.K. Park, J. Kiyan, T. Kirsch, I. Dumler, H. Haller, N. Shushakova, Renal urokinase-type plasminogen activator (uPA) receptor but not uPA deficiency strongly attenuates ischemia reperfusion injury and acute kidney allograft rejection, J. Immunol., 181 (2008) 1179-1189.
[48] C.L. Allen, U. Bayraktutan, Antioxidants attenuate hyperglycaemia-mediated brain endothelial cell dysfunction and blood-brain barrier hyperpermeability, Diabetes Obesity & Metabolism, 11 (2009) 480-490.
[49] C.L. Allen, U. Bayraktutan, Oxidative stress and its role in the pathogenesis of ischaemic stroke, Int. J. Stroke, 4 (2009) 461-470.
[50] C. Allen, K. Srivastava, U. Bayraktutan, Small GTPase RhoA and its effector rho kinase mediate oxygen glucose deprivation-evoked in vitro cerebral barrier dysfunction, Stroke, 41 (2010) 2056-2063.
[51] C.L. Gibson, K. Srivastava, N. Sprigg, P.M.W. Bath, U. Bayraktutan, inhibition of rho kinase protects cerebral barrier from ischaemia-evoked injury through modulations of endothelial cell oxidtive stress and tight junctions, J. Neurochem., 129 (2014) 816-826.
[52] Z. Abdullah, U. Bayraktutan, NADPH oxidase mediates TNF-alpha-evoked in vitro brain barrier dysfunction: roles of apoptosis and time, Mol. Cell. Neurosci., 61 (2014) 72-84.
[53] K. Srivastava, B. Shao, U. Bayraktutan, PKC-beta exacerbates in vitro brain barrier damage in hyperglycemic settings via regulation of RhoA/Rho-kinase/MLC2 pathway, J. Cereb. Blood Flow Metab., 33 (2013) 1928-1936.
[54] W. Hacke, G. Donnan, C. Fieschi, M. Kaste, R. von Kummer, J.P. Broderick, T. Brott, M. Frankel, J.C. Grotta, E.C. Haley, Jr., T. Kwiatkowski, S.R. Levine, C. Lewandowski, M. Lu, P. Lyden, J.R. Marler, S. Patel, B.C. Tilley, G. Albers, E. Bluhmki, M. Wilhelm, S. Hamilton, Association of outcome with early stroke treatment: pooled analysis of ATLANTIS, ECASS, and NINDS rt-PA stroke trials, Lancet, 363 (2004) 768-774.
[55] V. Thallas-Bonke, S.R. Thorpe, M.T. Coughlan, K. Fukami, F.Y.T. Yap, K.C. Sourris, S.A. Penfold, L.A. Bach, M.E. Cooper, J.M. Forbes, Inhibition of NADPH oxidase prevents advanced glycation end product-mediated damage in diabetic nephropathy through a protein kinase C-alpha-dependent pathway, Diabetes, 57 (2008) 460-469.
[56] H.G. Bohlen, G.P. Nase, Arteriolar nitric oxide concentration is decreased during hyperglycemia-induced beta II PKC activation, American Journal of Physiology-Heart and Circulatory Physiology, 280 (2001) H621-H627.

[57] A. Kouroedov, M. Eto, H. Joch, M. Volpe, T.F. Luscher, F. Cosentino, Selective inhibition of protein kinase C beta(2) prevents acute effects of high glucose on vascular cell adhesion molecule-1 expression in human endothelial cells, Circulation, 110 (2004) 91-96.
[58] G. Booth, T.J. Stalker, A.M. Lefer, R. Scalia, Mechanisms of amelioration of glucose-induced endothelial dysfunction following inhibition of protein kinase C in vivo, Diabetes, 51 (2002) 1556-1564.
[59] E. Oancea, T. Meyer, Protein kinase C as a molecular machine for decoding calcium and diacylglycerol signals, Cell, 95 (1998) 307-318.
[60] M. De Bock, M. Culot, N. Wang, A. da Costa, E. Decrock, M. Bol, G. Bultynck, R. Cecchelli, L. Leybaert, Low extracellular Ca2+ conditions induce an increase in brain endothelial permeability that involves intercellular Ca2+ waves, Brain Res., 1487 (2012) 78-87.
[61] J.G.N. Garcia, J. Stasek, V. Natarajan, C.E. Patterson, J. Dominguez, Role of protein-kinase-C in the regulation of prostaglandin synthesis in human endothelium, Am. J. Respir. Cell Mol. Biol., 6 (1992) 315-325.
[62] R. Brouns, P.P. De Deyn, The complexity of neurobiological processes in acute ischemic stroke, Clin. Neurol. Neurosurg., 111 (2009) 483-495.
[63] T.J. Degraba, P.T. Ostrow, R.A. Strong, R.M. Earls, Z.J. Zong, J.C. Grotta, Temporal relation of calcium-calmodulin binding and neuronal damage after global-ischemia in rats, Stroke, 23 (1992) 876-882.
[64] J.C. Grotta, C.M. Picone, J.R. Dedman, H.M. Rhoades, R.A. Strong, R.M. Earls, L.P. Yao, Neuronal protection correlates with prevention of calcium-calmodulin binding in rats, Stroke, 21 (1990) 28-31.
[65] H.J. Gelmers, M. Hennerici, Effect of nimodipine on acute ischemic stroke - pooled results from 5 randomized trials, Stroke, 21 (1990) 81-84.
[66] V. Holthoff, C. Beil, U. Hartmannklosterkotter, M. Neveling, G. Pawlik, K. Herholz, W.D. Heiss, Effect of nimodipine on glucose-metabolism in the course of ischemic stroke, Stroke, 21 (1990) 95-97.
[67] J. Horn, M. Limburg, Calcium antagonists for ischemic stroke - A systematic review, Stroke, 32 (2001) 570-576.
[68] J. Zhang, J. Yang, C. Zhang, X. Jiang, H. Zhou, M. Liu, Calcium antagonists for acute ischemic stroke, Cochrane Database of Systematic Reviews, (2012).
[69] Y. Persidsky, S.H. Ramirez, J. Haorah, G.D. Kanmogne, Blood-brain barrier: structural components and function under physiologic and pathologic conditions, J. Neuroimmune Pharmacol., 1 (2006) 223-236.
[70] Y. Hayashi, M. Nomura, S.I. Yamagishi, S.I. Harada, J. Yamashita, H. Yamamoto, Induction of various blood-brain barrier properties in non-neural endothelial cells by close apposition to co-cultured astrocytes, Glia, 19 (1997) 13-26.
[71] M.C. Nowycky, A.P. Fox, R.W. Tsien, 3 types of neuronal calcium-channel with different calcium agonist sensitivity, Nature, 316 (1985) 440-443.
[72] A.A. Mohamed, O. Gotoh, D.I. Graham, K.A. Osborne, J. McCulloch, A.D. Mendelow, G.M. Teasdale, A.M. Harper, Effect of pretreatment with the calcium-antagonist nimodipine on local cerebral blood-flow and histopathology after middle cerebral-artery occlusion, Ann. Neurol., 18 (1985) 705-711.
[73] W. Paschen, Disturbances of calcium homeostasis within the endoplasmic reticulum may contribute to the development of ischemic-cell damage, Med. Hypotheses, 47 (1996) 283-288.
[74] S. Fischer, M. Wiesnet, D. Renz, W. Schaper, H2O2 induces paracellular permeability of porcine brain-derived microvascular endothelial cells by activation of the p44/42 MAP kinase pathway, Eur. J. Cell Biol., 84 (2005) 687-697.

[75] M.Y. Ahn, Z.G. Zhang, W. Tsang, M. Chopp, Endogenous plasminogen activator expression after embolic focal cerebral ischemia in mice, Brain Res., 837 (1999) 169-176.
[76] H. Matthews, M. Ranson, J.D. Tyndall, M.J. Kelso, Synthesis and preliminary evaluation of amiloride analogs as inhibitors of the urokinase-type plasminogen activator (uPA), Bioorg. Med. Chem. Lett., 21 (2011) 6760-6766.
[77] H. Tang, D.M. Kerins, Q. Hao, T. Inagami, D.E. Vaughan, The urokinase-type plasminogen activator receptor mediates tyrosine phosphorylation of focal adhesion proteins and activation of mitogen-activated protein kinase in cultured endothelial cells, J. Biol. Chem., 273 (1998) 18268-18272.
[78] E. Lengyel, H. Wang, R. Gum, C. Simon, Y. Wang, D. Boyd, Elevated urokinase-type plasminogen activator receptor expression in a colon cancer cell line is due to a constitutively activated extracellular signal-regulated kinase-1-dependent signaling cascade, Oncogene, 14 (1997) 2563-2573.
[79] K. Nakajima, Y. Tohyama, S. Kohsaka, T. Kurihara, Protein kinase C alpha requirement in the activation of p38 mitogen-activated protein kinase, which is linked to the induction of tumor necrosis factor alpha in lipopolysaccharide-stimulated microglia, Neurochem. Int., 44 (2004) 205-214.
[80] G. Fibbi, R. Caldini, M. Chevanne, M. Pucci, N. Schiavone, L. Morbidelli, A. Parenti, H.J. Granger, M. Del Rosso, M. Ziche, Urokinase-dependent angiogenesis in vitro and diacylglycerol production are blocked by antisense oligonucleotides against the urokinase receptor, Lab. Invest., 78 (1998) 1109-1119.
[81] R.G. Sitrin, P.M. Pan, H.A. Harper, R.A. Blackwood, R.F. Todd, Urokinase receptor (CD87) aggregation triggers phosphoinositide hydrolysis and intracellular calcium mobilization in mononuclear phagocytes, J. Immunol., 163 (1999) 6193-6200.
[82] S.P. Christow, R. Bychkov, C. Schroeder, R. Dietz, H. Haller, I. Dumler, D.C. Gulba, Urokinase activates calcium-dependent potassium channels in U937 cells via calcium release from intracellular stores, Eur. J. Biochem., 265 (1999) 264-272.
[83] A. Espinosa, A. Garcia, S. Haertel, C. Hidalgo, E. Jaimovich, NADPH Oxidase and Hydrogen Peroxide Mediate Insulin-induced Calcium Increase in Skeletal Muscle Cells, J. Biol. Chem., 284 (2009) 2568-2575.
[84] Q.H. Hu, Z.X. Yu, V.J. Ferrans, K. Takeda, K. Irani, R.C. Ziegelstein, Critical role of NADPH oxidase-derived reactive oxygen species in generating Ca2+ oscillations in human aortic endothelial cells stimulated by histamine, J. Biol. Chem., 277 (2002) 32546-32551.
[85] Q.H. Hu, G.M. Zheng, J.L. Zweier, S. Deshpande, K. Irani, R.C. Ziegelstein, NADPH oxidase activation increases the sensitivity of intracellular Ca2+ stores to inositol 1,4,5-trisphosphate in human endothelial cells, J. Biol. Chem., 275 (2000) 15749-15757.
[86] D. Pandey, J.-P. Gratton, R. Rafikov, S.M. Black, D.J.R. Fulton, Calcium/Calmodulin-Dependent Kinase II Mediates the Phosphorylation and Activation of NADPH Oxidase 5, Mol. Pharmacol., 80 (2011) 407-415.
[87] J.M. Cook-Mills, J.D. Johnson, T.L. Deem, A. Ochi, L. Wang, Y. Zheng, Calcium mobilization and Rac1 activation are required for VCAM-1 (vascular cell adhesion molecule-1) stimulation of NADPH oxidase activity, Biochem. J., 378 (2004) 539-547.
[88] S. Umemoto, M. Tanaka, S. Kawahara, M. Kubo, K. Umeji, R. Hashimoto, M. Matsuzaki, Calcium antagonist reduces oxidative stress by upregulating Cu/Zn superoxide dismutase in stroke-prone spontaneously hypertensive rats, Hypertens. Res., 27 (2004) 877-885.
[89] R.P. Mason, P.R. Leeds, R.F. Jacob, C.J. Hough, K.G. Zhang, P.E. Mason, D.M. Chuang, Inhibition of excessive neuronal apoptosis by the calcium antagonist amlodipine and antioxidants in cerebellar granule cells, J. Neurochem., 72 (1999) 1448-1456.

[90] N.R. Sims, M.F. Anderson, Mitochondrial contributions to tissue damage in stroke, Neurochem. Int., 40 (2002) 511-526.
[91] R. Gopalakrishna, S. Jaken, Protein kinase C signaling and oxidative stress, Free Radic. Biol. Med., 28 (2000) 1349-1361.
[92] H. Raad, M.-H. Paclet, T. Boussetta, Y. Kroviarski, F. Morel, M.T. Quinn, M.-A. Gougerot-Pocidalo, P.M.-C. Dang, J. El-Benna, Regulation of the phagocyte NADPH oxidase activity: phosphorylation of gp91(phox)/NOX2 by protein kinase C enhances its diaphorase activity and binding to Rac2, p67(phox), and p47(phox), FASEB J., 23 (2009) 1011-1022.
[93] A. Fontayne, P.M.C. Dang, M.A. Gougerot-Pocidalo, J. El Benna, Phosphorylation of p47(phox) sites by PKC alpha, beta II, delta, and zeta: Effect on binding to p22(phox) and on NADPH oxidase activation, Biochemistry, 41 (2002) 7743-7750.
[94] S.R. Lee, E.H. Lo, Induction of caspase-mediated cell death by matrix metalloproteinases in cerebral endothelial cells after hypoxia-reoxygenation, J. Cereb. Blood Flow Metab., 24 (2004) 720-727.
[95] E.A. Hixenbaugh, Z.M. Goeckeler, N.N. Papaiya, R.B. Wysolmerski, S.C. Silverstein, A.J. Huang, Stimulated neutrophils induce myosin light chain phosphorylation and isometric tension in endothelial cells, American Journal of Physiology-Heart and Circulatory Physiology, 273 (1997) H981-H988.
[96] R.J. Korthuis, D.L. Carden, P.R. Kvietys, D. Shepro, J. Fuseler, Phalloidin attenuates postischemic neutrophil infiltration and increased microvascular permeability, J. Appl. Physiol., 71 (1991) 1261-1269.
[97] H. Lum, K.A. Roebuck, Oxidant stress and endothelial cell dysfunction, American Journal of Physiology-Cell Physiology, 280 (2001) C719-C741.
[98] H. Alluri, H.W. Stagg, R.L. Wilson, R.P. Clayton, D.A. Sawant, M. Koneru, M.R. Beeram, M.L. Davis, B. Tharakan, Reactive Oxygen Species-Caspase-3 Relationship in Mediating Blood-Brain Barrier Endothelial Cell Hyperpermeability Following Oxygen-Glucose Deprivation and Reoxygenation, Microcirculation, 21 (2014) 187-195.

7. Figure Legends

Figure 1 – 1 column

Shorter periods of OGD±R result in increases in intracellular calcium levels and caspase-3/7 activity. HBMEC were exposed to 30 mins, 1 hour, 2 hours or 4 hours of OGD alone or followed by 20 hours of reperfusion (R). Intracellular calcium levels (A) and caspase-3/7 activity (B) are increased compared to normoxic cells in all OGD±R conditions. Data represented as mean ± SEM from $n \geq 4$. * $P < 0.05$ compared to Normoxia. † $P < 0.05$ compared to respective OGD group.

Figure 2 – 2 column

Shorter periods of OGD±R result in increases the rate of apoptosis. HBMEC were exposed to 30 mins, 1 hour, 2 hours or 4 hours of OGD alone or followed by 20 hours of reperfusion (R). The rate of apoptosis was increased during all OGD±R time points compared to normoxic cells (A). TUNEL staining showed an increase in the number of apoptotic nuclei (dark brown staining) in all OGD±R conditions compared to normoxic cells (Bar 50 μm, B). Arrows indicate representative apoptotic nuclei. Data represented as mean ± SEM from n = 4. * $P < 0.05$ compared to Normoxia.

Figure 3 – 2 column

PKC-α is a key player in increasing total PKC activity during OGD±R. HBMEC were exposed to 4 hours OGD (OGD) with or without reperfusion (R) or a PKC activator PMA. Bisindolylmaleimide, a general PKC activity inhibitor, normalised the increases in PKC activity seen during OGD±R (A). Inhibitors for α (Ro-32-0432), β (LY-333531) and β_{II} (CGP-53353) isoforms also show attenuation of increased PKC activity during OGD±R (B). PKC-α (C) and PKC-β_I (D) activities are increased during OGD±R. Chelation of intracellular calcium with BAPTA-AM decreased the rise in PKC activity seen during OGD±R (E). PMA increased PKC activity and co-exposure or 4 hours pre-exposure with BAPTA-AM normalised the increases seen (F). Exposure to PMA also increased PKC-α activity (G). Data

represented as mean ± SEM from ≥ 3. * $P < 0.05$ compared to Normoxia or control. † $P < 0.05$ compared to respective untreated group. § $P < 0.05$ compared to PMA.

Figure 4 – 2 column

Amiloride and apocynin reduce PKC activity and uPA activity affected by PKC-α. HBMEC were exposed to 4 hours OGD (OGD) with or without reperfusion (R) in the absence or presence of inhibitors for uPA (amiloride), NADPH oxidase (apocynin), intracellular calcium (BAPTA-AM) or PKC-α (RO-32-0432). Amiloride and apocynin decreased the rise in total PKC (A) and PKC-α (B) activities seen during OGD±R. tPA activity is increased during OGD±R and treatment with BAPT-AM and RO-32-0432 show no effect (C). uPA activity is also increased during OGD±R and BAPTA-AM and RO-32-0432 normalised the increases seen (D). Data represented as mean ± SEM from n ≥ 3. * $P < 0.05$ compared to Normoxia. † $P < 0.05$ compared to respective untreated group.

Figure 5 – 2 column

PKC-α reduces total $O_2^{\bullet-}$ levels and NADPH activity. HBMEC were exposed to 4 hours OGD (OGD) with or without reperfusion (R) in the absence or presence of inhibitors for PKC (bisindolylmaleimide), intracellular calcium (BAPTA-AM) or PKC-α (RO-32-0432). HBMEC were also exposed to PMA, a PKC activator, with or without BAPTA-AM treatment. Total $O_2^{\bullet-}$ levels were increased during OGD±R and treatment with bisindolylmaleimide or RO-32-0432 normalised $O_2^{\bullet-}$ levels although they remained higher than normoxic cells (A). Treatment with BAPTA-AM completely normalised the increases observed (B). NADPH oxidase activity followed a similar pattern to that of $O_2^{\bullet-}$ levels during OGD±R (C-D). Exposure to PMA increased $O_2^{\bullet-}$ levels and NADPH oxidase activity and treatment with BAPTA-AM abolished these changes (E-F). Data represented as mean ± SEM from n ≥ 3. * $P < 0.05$ compared to Normoxia or control. § $P < 0.05$ compared to 4 hrs OGD. † $P < 0.05$ compared to respective untreated group.

Figure 6 – 1.5 column

Inhibition of NADPH oxidase, PKC-α, and uPA reduces OGD±R induced increases in caspase-3/7 activity and apoptosis rate. HBMEC were exposed to 4 hours OGD (OGD) with or without reperfusion (R) in the absence or presence of inhibitors for uPA (amiloride), NADPH oxidase (apocynin), intracellular calcium (BAPTA-AM) or PKC-α (RO-32-0432). Amiloride and apocynin reduced increases in intracellular calcium levels during reperfusion only whereas BAPTA-AM reduced calcium levels during OGD±R. RO-32-0432 reduced calcium levels during OGD±R although levels remained elevated compared to normoxic cells especially during OGD (A). Amiloride and apocynin reduced the increase observed in caspase-3/7 activity during OGD±R however activity still remained higher than normoxic cells during reperfusion. Both BAPTA-AM and RO-32-0432 normalised caspase-3/7 activities during OGD±R (B). Data represented as mean ± SEM from n ≥ 3. * $P < 0.05$ compared to Normoxia. † $P < 0.05$ compared to respective untreated group.

Figure 7 – 1 column

Knockdown of PKC-α reduces PKC-α protein levels. PKC-α knockdown reduces PKC-α protein levels compared to control cells and cells exposed to non-targeting (NT) siRNA as confirmed by Western blotting. Data represented as mean ± SEM from n = 4. * $P < 0.05$ compared to control.

Figure 8 – 2 column

Knockdown of PKC-α reduces OGD±R induced increases in caspase-3/7 activity and apoptosis rate. HBMEC were exposed to 4 hours OGD (OGD) with or without reperfusion (R) in the absence or presence of PKC-α siRNA. PKC-α knockdown cells reduced caspase-3/7 activity and the rate of apoptosis compared to untreated cells (A and B). TUNEL staining for PKC-α knockdown cells exposed to OGD±R showed fewer apoptotic nuclei (dark brown staining) compared to NT siRNA treated cells (Bar 50 μm, C). Arrows indicate representative apoptotic nuclei. Data represented as mean ± SEM from n ≥ 3. * $P < 0.05$ compared to Normoxia. † $P < 0.05$ compared to respective untreated group.

Figure 9 – 2 column

Amiloride, apocynin, BAPTA-AM and RO-32-0432 reduced the rate of apoptosis. HBMEC were exposed to 4 hours OGD (OGD) with or without reperfusion (R) in the absence or presence of inhibitors for uPA (amiloride), NADPH oxidase (apocynin), intracellular calcium (BAPTA-AM) or PKC-α (RO-32-0432). All inhibitors showed a reduced rate of apoptosis during OGD±R however the rate remained elevated compared to normoxic cells (A). TUNEL staining showed fewer apoptotic nuclei (dark brown staining) compared to untreated cells (Bar 50 μm, B). Arrows indicate representative apoptotic nuclei. Data represented as mean ± SEM from $n \geq 4$. * $P < 0.05$ compared to Normoxia. † $P < 0.05$ compared to respective untreated group.

Figure 10 - 2 column

OGD±R increases stress fibre formation. HBMEC were grown on coverslips and exposed to 4 hours OGD (OGD) with or without reperfusion (R) in the absence or presence of inhibitors for uPA (amiloride), NADPH oxidase (apocynin), intracellular calcium (BAPTA-AM) or PKC-α (RO-32-0432). Cells targeted with PKC-α siRNA or non-targeting (NT) siRNA were also exposed to the above conditions. Cells were stained with rhodamine phalloidin to visualise F-actin. Cells exposed to OGD±R showed stress fibre formation compared to normoxic cells and treated cells showed less stress fibre formation compared to untreated cells exposed to OGD±R (bar 50 μm). Data represented from $n \geq 4$.

Figure 11 – 2 column

PKC-α knockdown restores BBB integrity after OGD±R. HBMEC and HA co-cultures were exposed to 4 hours OGD (OGD) with or without reperfusion (R) in the absence or presence of BAPTA-AM, an intracellular calcium inhibitor. Co-cultures were also exposed to PMA, a PKC activator ± BAPTA-AM. HBMEC targeted with PKC-α siRNA or NT siRNA in co-culture with HA were also exposed to the above OGD±R or PMA conditions. Co-cultures exposed to OGD±R reperfusion with BAPTA-AM show higher TEER values and lower EBA and NaF flux volumes compared to co-cultures exposed to OGD±R alone (A). PKC-α knockdown increases TEER and decreases EBA and NaF flux compared to co-cultures

exposed to OGD±R alone (D-F). PMA increases BBB permeability which is normalised with BAPTA-AM and PKC-α knockdown (G-I). Data represented as mean ± SEM from n ≥ 4. * $P < 0.05$ compared to Normoxia. § $P < 0.05$ compared to respective 4 hrs OGD exposed cells. † $P < 0.05$ compared to respective untreated group. ‡ $P < 0.05$ compared to respective NT siRNA targeted group. ∞ $P < 0.05$ compared to PMA. Ψ $P < 0.05$ compared to PMA with NT siRNA.

A

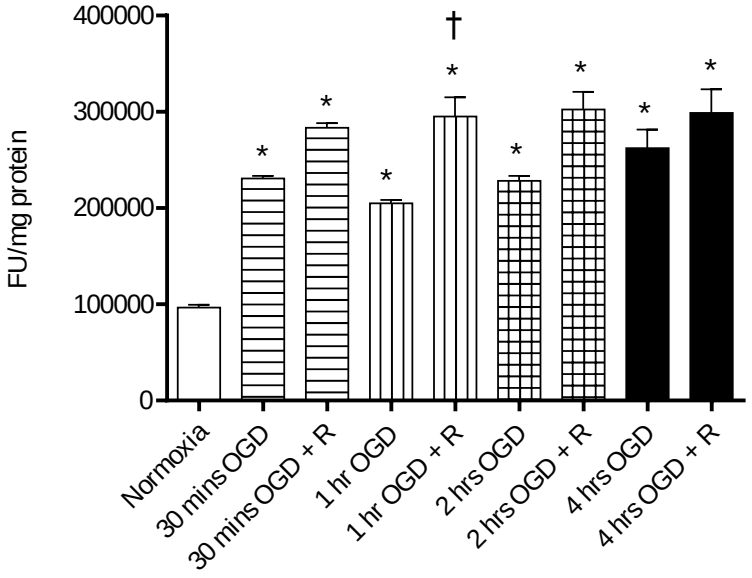
400000
300000
200000
100000
0
FU/mg protein
†
*
Normoxia
30 mins OGD
30 mins OGD + R
1 hr OGD
1 hr OGD + R
2 hrs OGD
2 hrs OGD + R
4 hrs OGD
4 hrs OGD + R

B

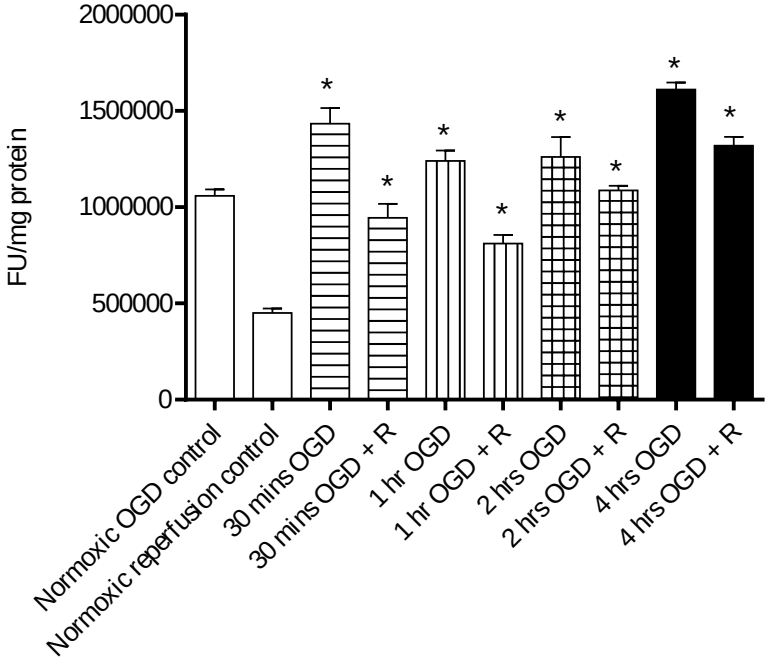
2000000
1500000
1000000
500000
0
FU/mg protein
*
Normoxic OGD control
Normoxic reperfusion control
30 mins OGD
30 mins OGD + R
1 hr OGD
1 hr OGD + R
2 hrs OGD
2 hrs OGD + R
4 hrs OGD
4 hrs OGD + R

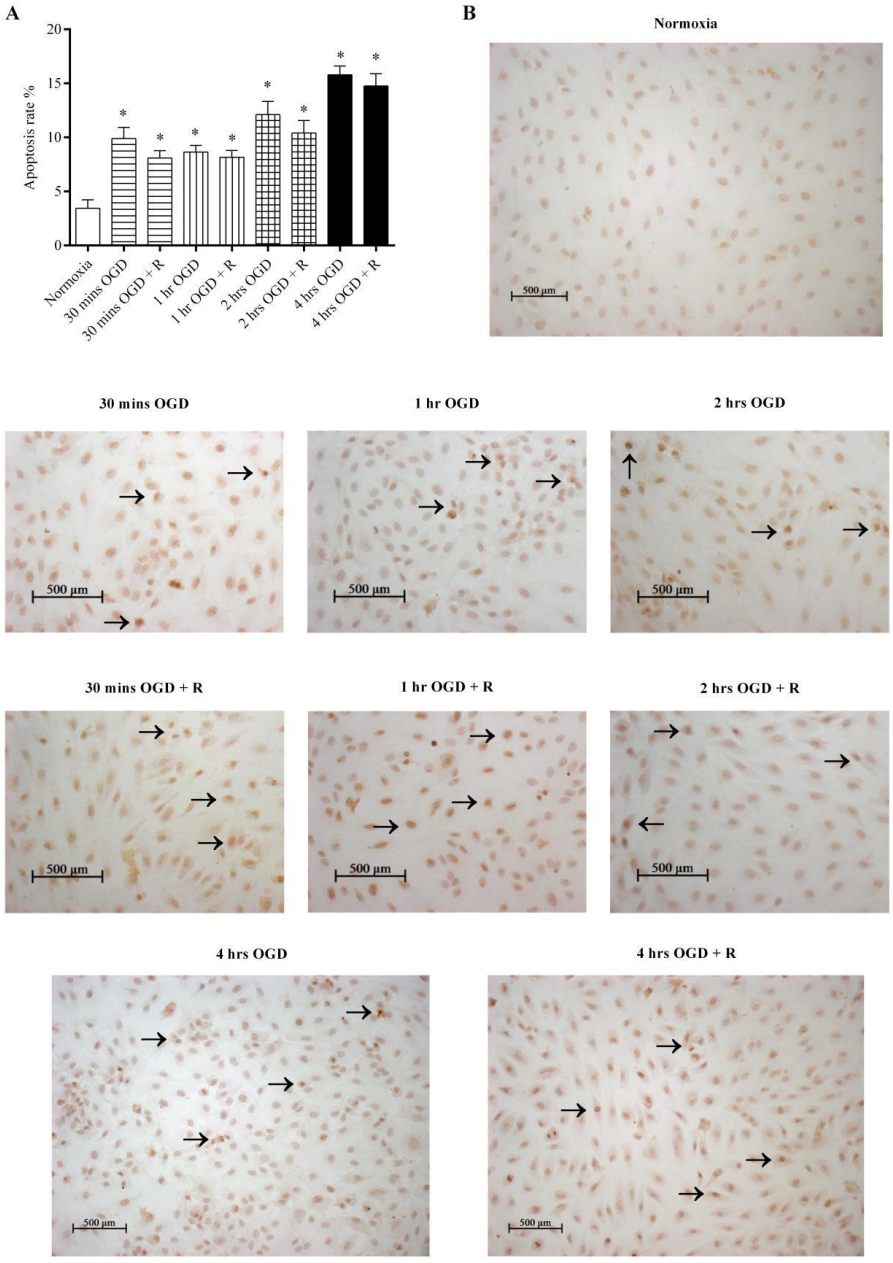
A
Apoptosis rate %
20
15
10
5
0
Normoxia
30 mins OGD
30 mins OGD + R
1 hr OGD
1 hr OGD + R
2 hrs OGD
2 hrs OGD + R
4 hrs OGD
4 hrs OGD + R
B
Normoxia
30 mins OGD
1 hr OGD
2 hrs OGD
30 mins OGD + R
1 hr OGD + R
2 hrs OGD + R
4 hrs OGD
4 hrs OGD + R
500 μm

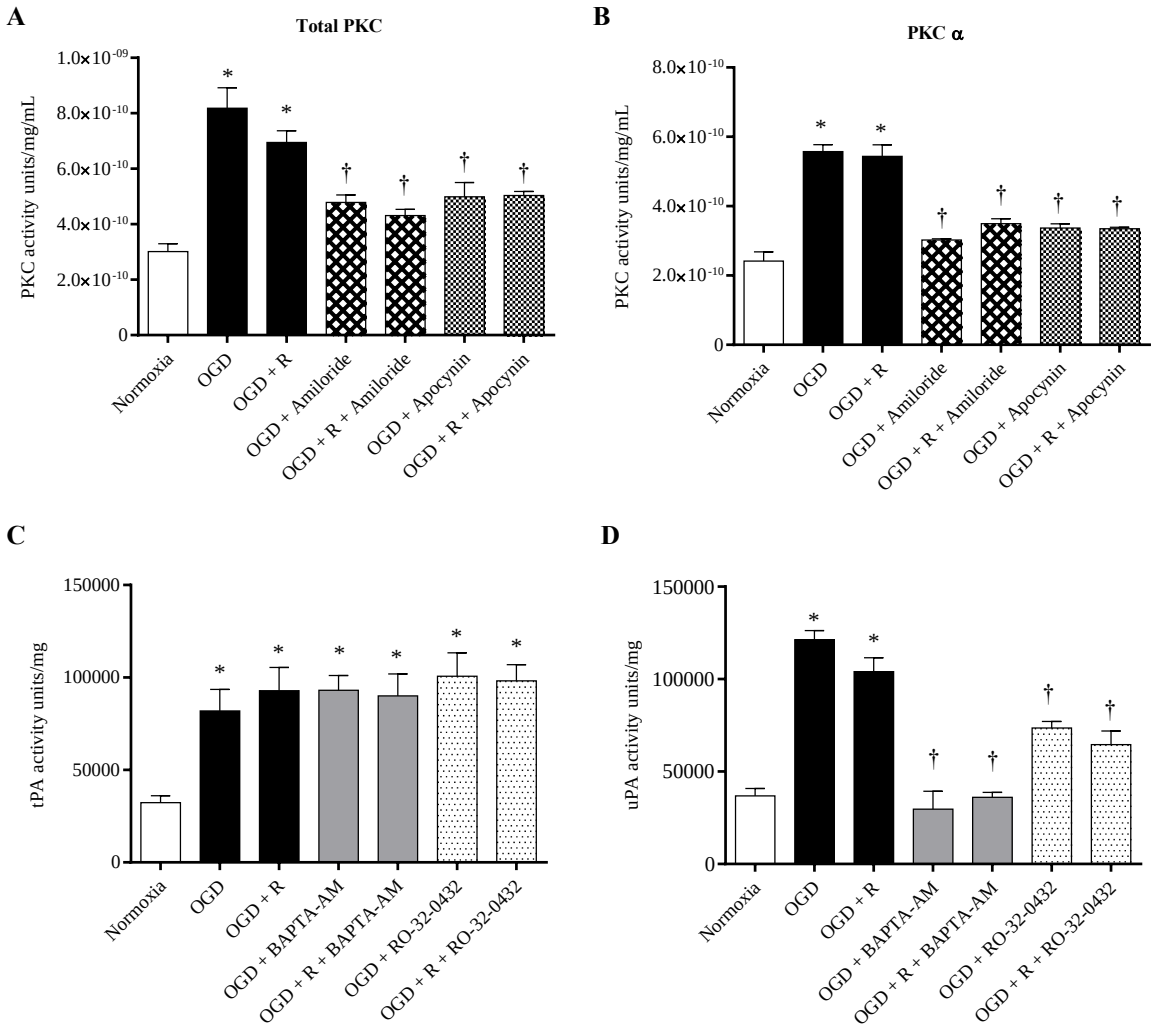
A
Total PKC
PKC activity units/mg/mL
1.0×10-09
8.0×10-10
6.0×10-10
4.0×10-10
2.0×10-10
0
Normoxia
OGD
OGD + R
OGD + Amiloride
OGD + R + Amiloride
OGD + Apocynin
OGD + R + Apocynin
B
PKC α
PKC activity units/mg/mL
8.0×10-10
6.0×10-10
4.0×10-10
2.0×10-10
0
C
tPA activity units/mg
150000
100000
50000
0
OGD + BAPTA-AM
OGD + R + BAPTA-AM
OGD + RO-32-0432
OGD + R + RO-32-0432
D
uPA activity units/mg

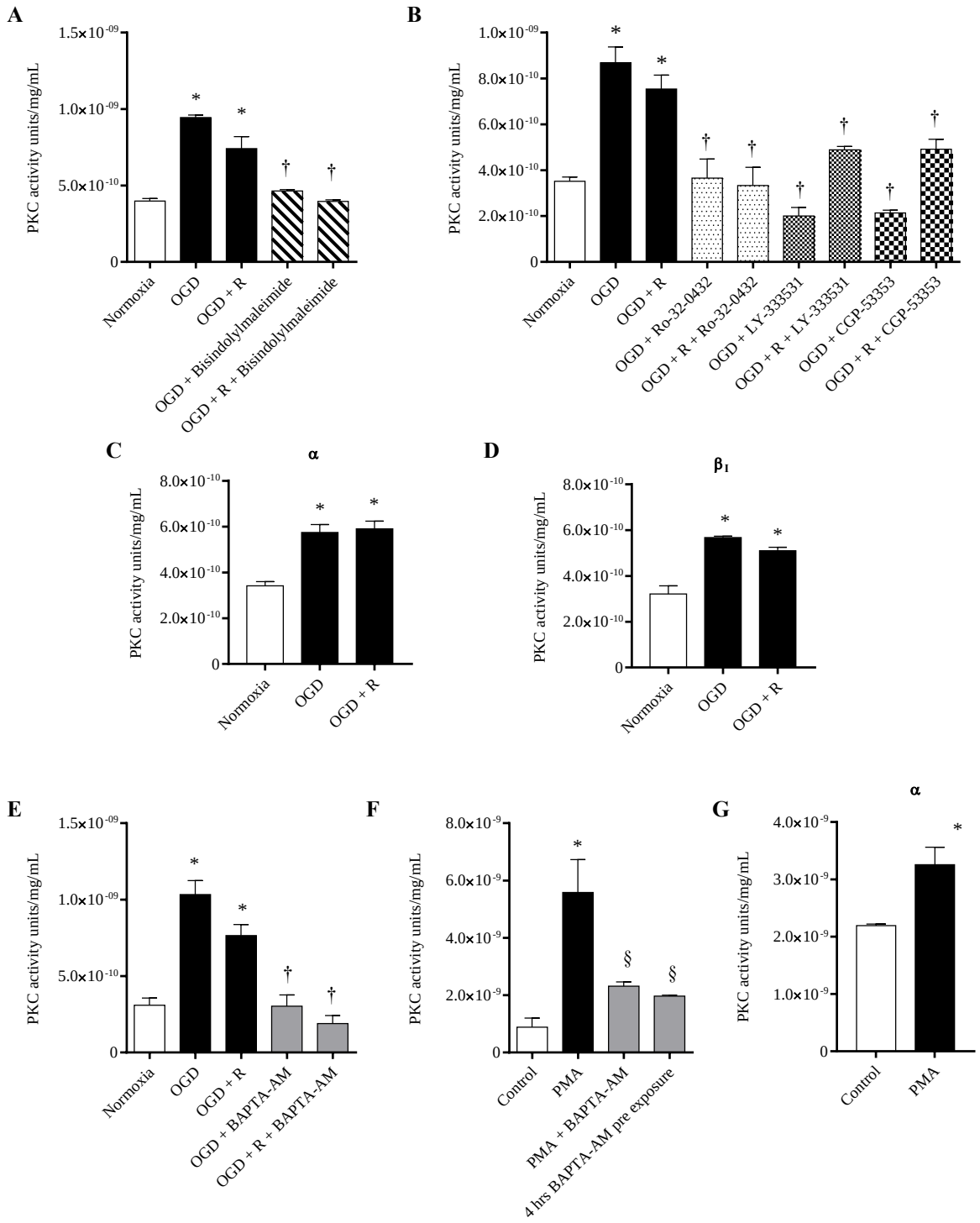
A
PKC activity units/mg/mL
1.5×10-09
1.0×10-09
5.0×10-10
0
Normoxia
OGD
OGD + R
OGD + Bisindolylmaleimide
OGD + R + Bisindolylmaleimide
B
PKC activity units/mg/mL
1.0×10-09
8.0×10-10
6.0×10-10
4.0×10-10
2.0×10-10
0
Normoxia
OGD
OGD + R
OGD + Ro-32-0432
OGD + R + Ro-32-0432
OGD + LY-333531
OGD + R + LY-333531
OGD + CGP-53353
OGD + R + CGP-53353
C
α
PKC activity units/mg/mL
8.0×10-10
6.0×10-10
4.0×10-10
2.0×10-10
0
Normoxia
OGD
OGD + R
D
βI
PKC activity units/mg/mL
8.0×10-10
6.0×10-10
4.0×10-10
2.0×10-10
0
Normoxia
OGD
OGD + R
E
PKC activity units/mg/mL
1.5×10-09
1.0×10-09
5.0×10-10
0
Normoxia
OGD
OGD + R
OGD + BAPTA-AM
OGD + R + BAPTA-AM
F
PKC activity units/mg/mL
8.0×10-9
6.0×10-9
4.0×10-9
2.0×10-9
0
Control
PMA
PMA + BAPTA-AM
4 hrs BAPTA-AM pre exposure
G
α
PKC activity units/mg/mL
4.0×10-9
3.0×10-9
2.0×10-9
1.0×10-9
0
Control
PMA

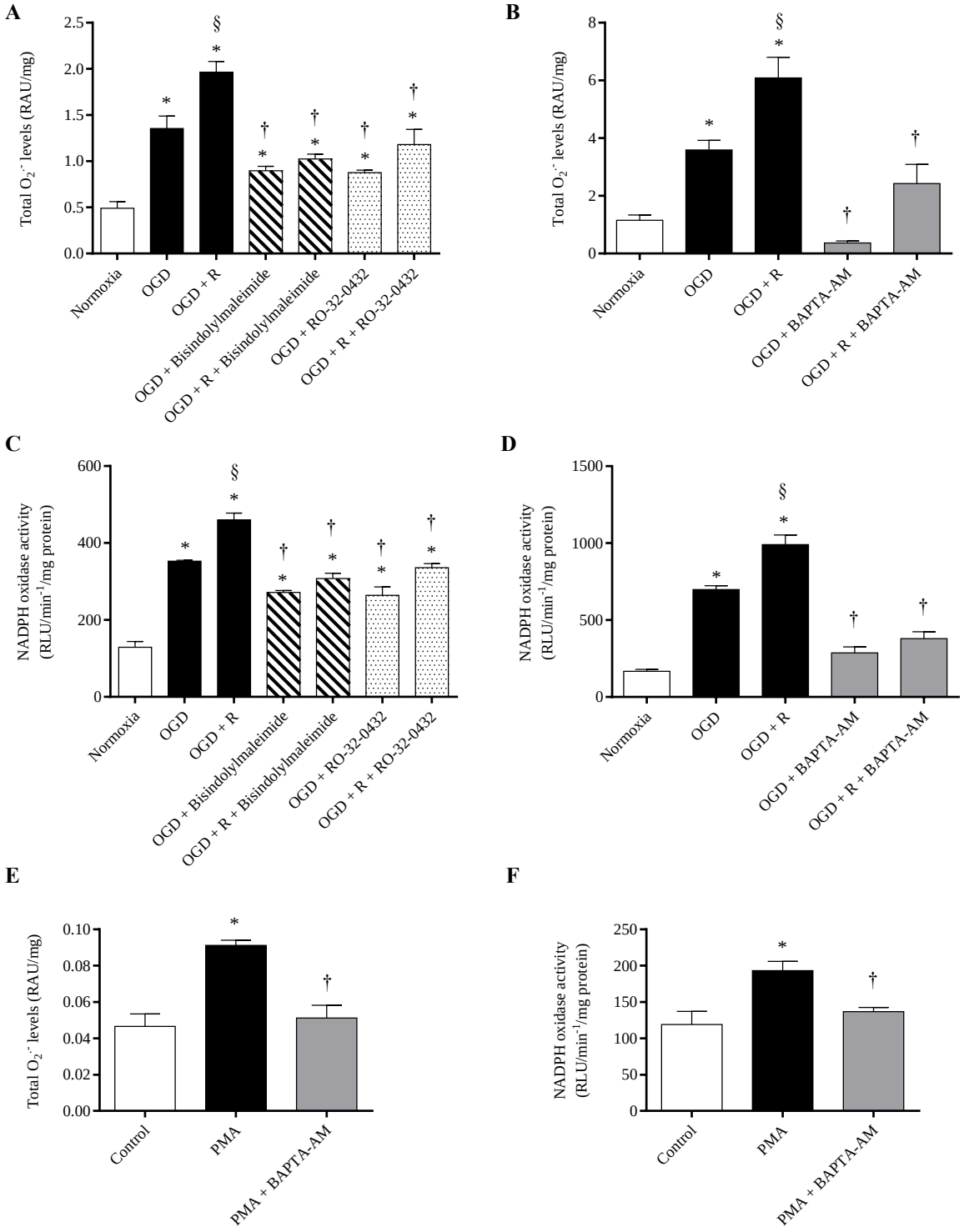
A
Total $O_2^{\cdot-}$ levels (RAU/mg)
2.5
2.0
1.5
1.0
0.5
0.0
Normoxia
OGD
OGD + R
OGD + Bisindolylmaleimide
OGD + R + Bisindolylmaleimide
OGD + RO-32-0432
OGD + R + RO-32-0432
B
Total $O_2^{\cdot-}$ levels (RAU/mg)
8
6
4
2
0
Normoxia
OGD
OGD + R
OGD + BAPTA-AM
OGD + R + BAPTA-AM
C
NADPH oxidase activity (RLU/min^{-1}/mg protein)
600
400
200
0
Normoxia
OGD
OGD + R
OGD + Bisindolylmaleimide
OGD + R + Bisindolylmaleimide
OGD + RO-32-0432
OGD + R + RO-32-0432
D
NADPH oxidase activity (RLU/min^{-1}/mg protein)
1500
1000
500
0
Normoxia
OGD
OGD + R
OGD + BAPTA-AM
OGD + R + BAPTA-AM
E
Total $O_2^{\cdot-}$ levels (RAU/mg)
0.10
0.08
0.06
0.04
0.02
0.00
Control
PMA
PMA + BAPTA-AM
F
NADPH oxidase activity (RLU/min^{-1}/mg protein)
250
200
150
100
50
0
Control
PMA
PMA + BAPTA-AM

A

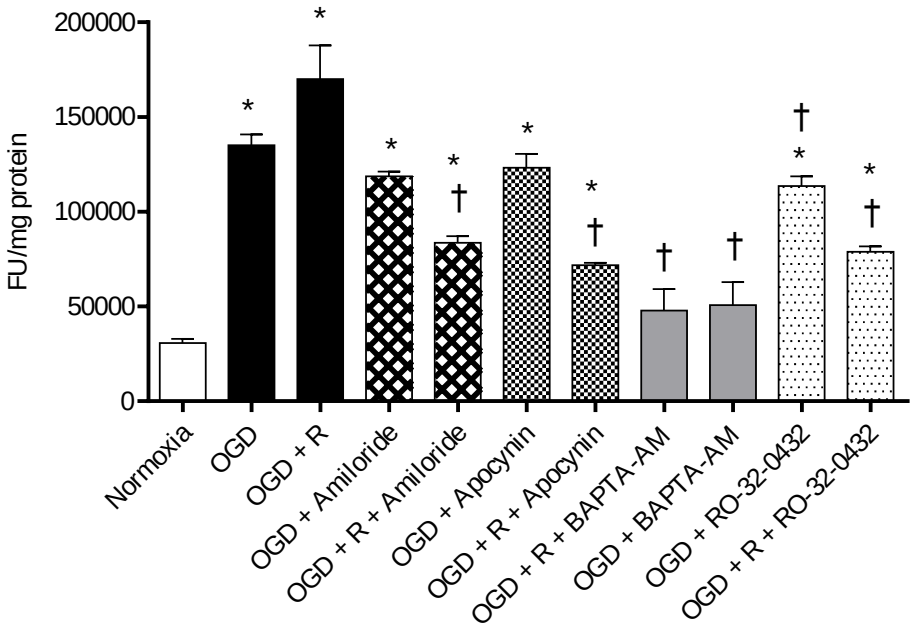
FU/mg protein
200000
150000
100000
50000
0
Normoxia
OGD
OGD + R
OGD + Amiloride
OGD + R + Amiloride
OGD + Apocynin
OGD + R + Apocynin
OGD + R + BAPTA-AM
OGD + BAPTA-AM
OGD + RO-32-0432
OGD + R + RO-32-0432

B

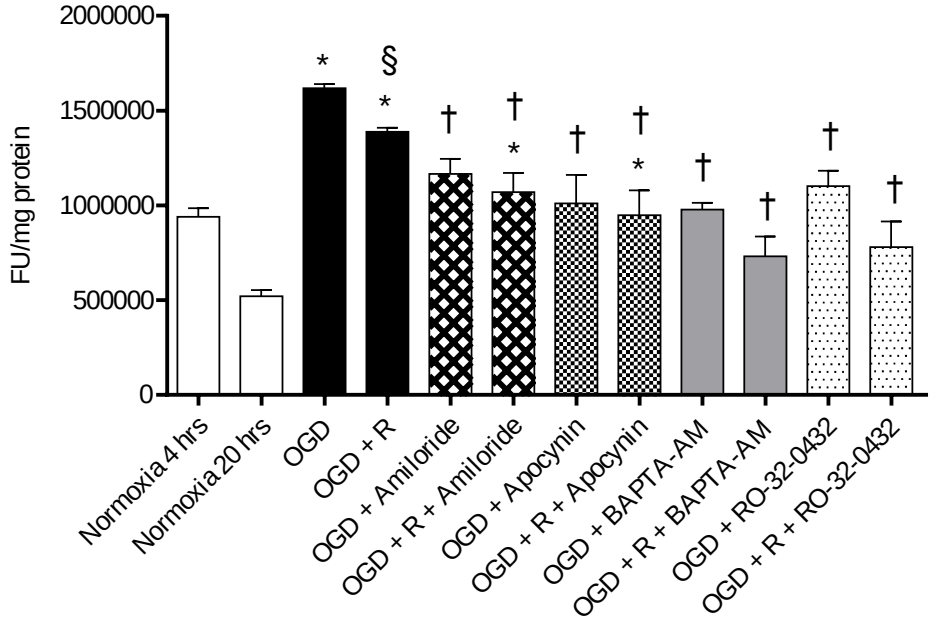
FU/mg protein
2000000
1500000
1000000
500000
0
Normoxia 4 hrs
Normoxia 20 hrs
OGD
OGD + R
OGD + Amiloride
OGD + R + Amiloride
OGD + Apocynin
OGD + R + Apocynin
OGD + BAPTA-AM
OGD + R + BAPTA-AM
OGD + RO-32-0432
OGD + R + RO-32-0432

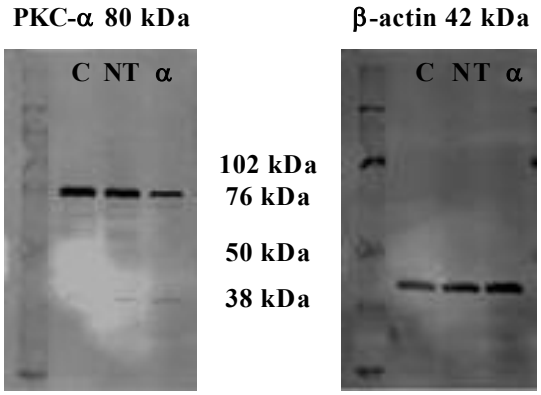
PKC-α 80 kDa
β-actin 42 kDa
C NT α
C NT α
102 kDa
76 kDa
50 kDa
38 kDa

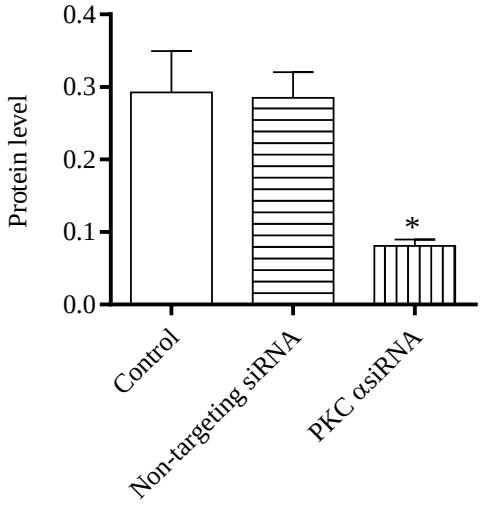
Protein level
0.4
0.3
0.2
0.1
0.0
*
Control
Non-targeting siRNA
PKC αsiRNA

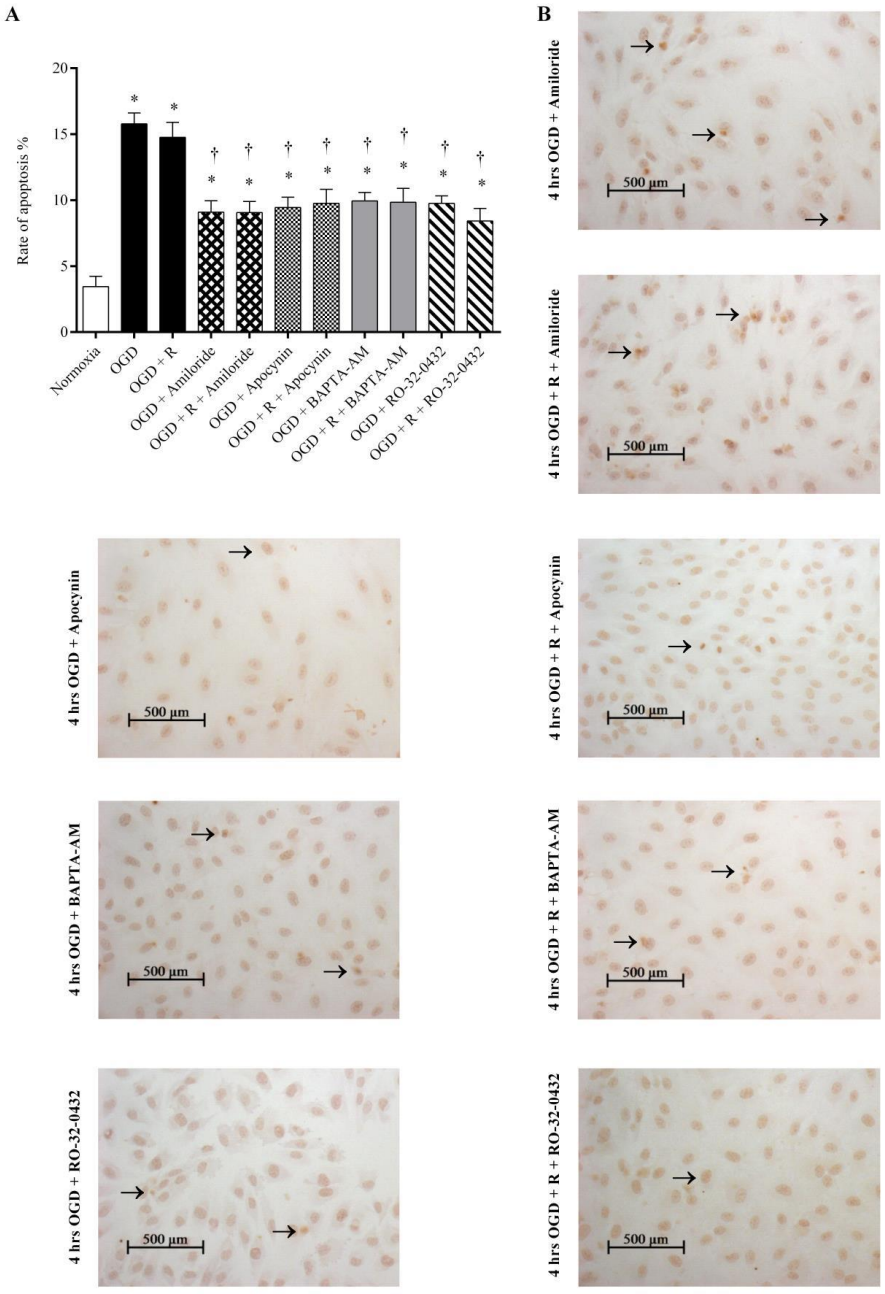
A
B
Rate of apoptosis %
20
15
10
5
0
Normoxia
OGD
OGD + R
OGD + Amiloride
OGD + R + Amiloride
OGD + Apocynin
OGD + R + Apocynin
OGD + BAPTA-AM
OGD + R + BAPTA-AM
OGD + RO-32-0432
OGD + R + RO-32-0432
4 hrs OGD + Amiloride
4 hrs OGD + R + Amiloride
4 hrs OGD + Apocynin
4 hrs OGD + R + Apocynin
4 hrs OGD + BAPTA-AM
4 hrs OGD + R + BAPTA-AM
4 hrs OGD + RO-32-0432
4 hrs OGD + R + RO-32-0432
500 μm

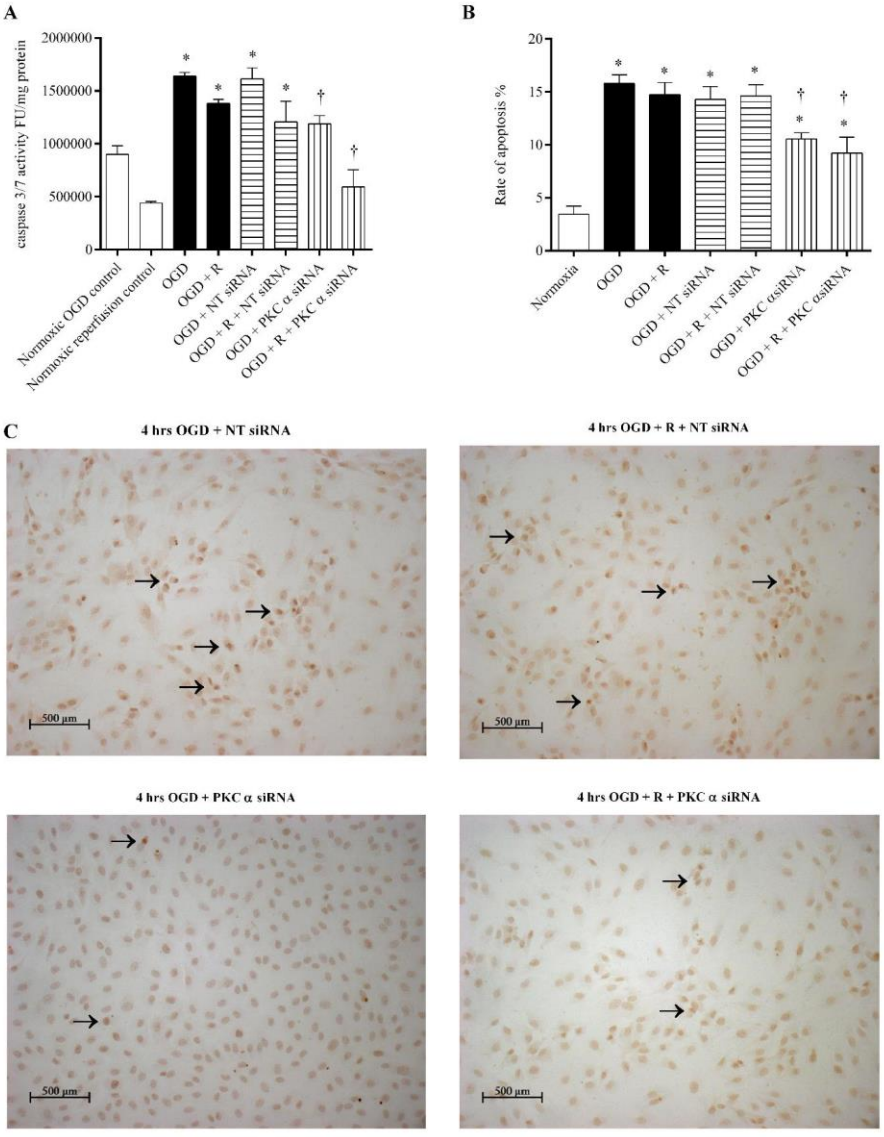
A
caspase 3/7 activity FU/mg protein
2000000
1500000
1000000
500000
0
Normoxic OGD control
Normoxic reperfusion control
OGD
OGD + R
OGD + NT siRNA
OGD + R + NT siRNA
OGD + PKC α siRNA
OGD + R + PKC α siRNA
B
Rate of apoptosis %
20
15
10
5
0
Normoxia
OGD
OGD + R
OGD + NT siRNA
OGD + R + NT siRNA
OGD + PKC αsiRNA
OGD + R + PKC αsiRNA
C
4 hrs OGD + NT siRNA
4 hrs OGD + R + NT siRNA
4 hrs OGD + PKC α siRNA
4 hrs OGD + R + PKC α siRNA
500 µm

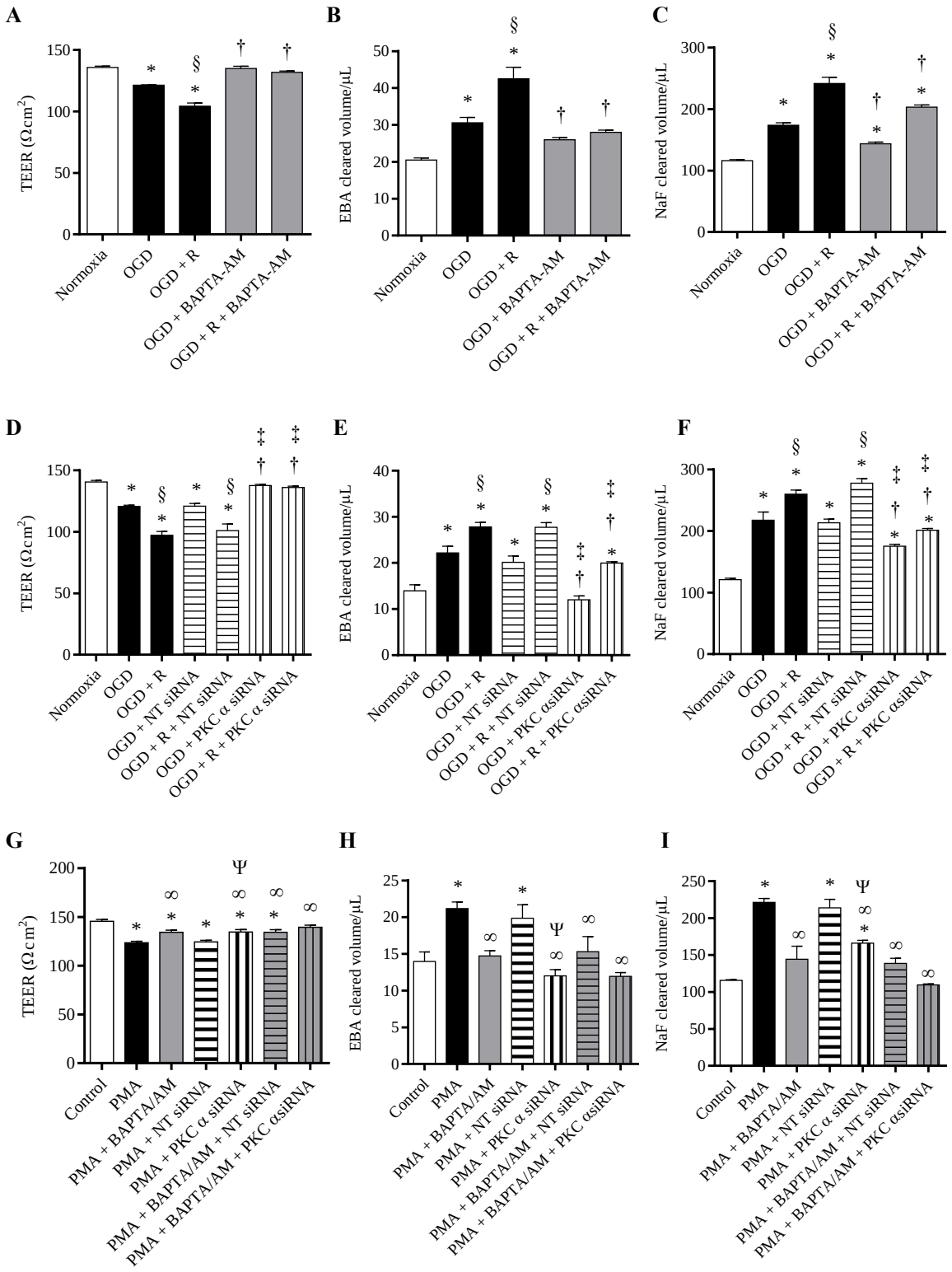
A
TEER (Ωcm²)
Normoxia
OGD
OGD + R
OGD + BAPTA-AM
OGD + R + BAPTA-AM
B
EBA cleared volume/μL
C
NaF cleared volume/μL
D
OGD + NT siRNA
OGD + R + NT siRNA
OGD + PKC α siRNA
OGD + R + PKC α siRNA
E
OGD + PKC αsiRNA
OGD + R + PKC αsiRNA
F
G
Control
PMA
PMA + BAPTA/AM
PMA + NT siRNA
PMA + PKC α siRNA
PMA + BAPTA/AM + NT siRNA
PMA + BAPTA/AM + PKC αsiRNA
H
I

Normoxia

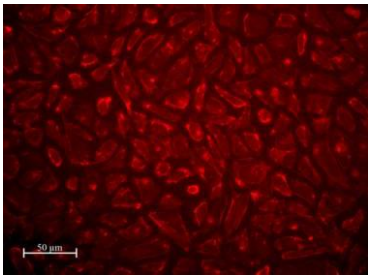

4 hrs OGD

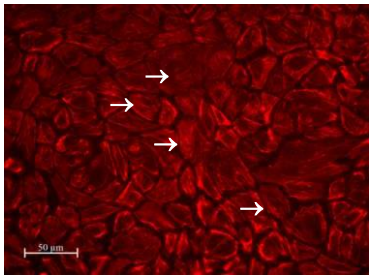

4 hrs OGD + R

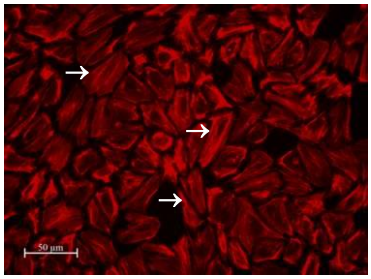

4 hrs OGD + Amiloride

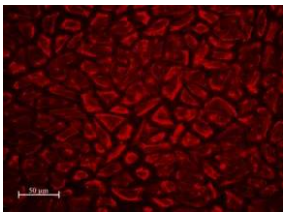

4 hrs OGD + R + Amiloride

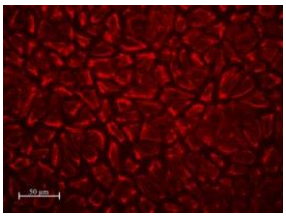

4 hrs OGD + Apocynin

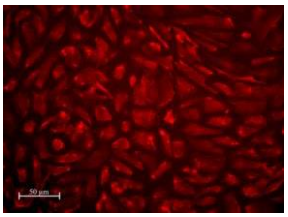

4 hrs OGD + R + Apocynin

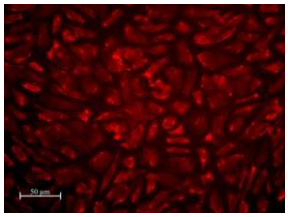

4 hrs OGD + BAPTA-AM

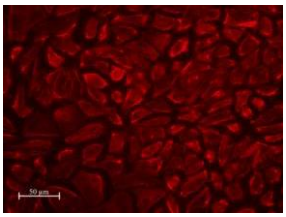

4 hrs OGD + R + BAPTA-AM

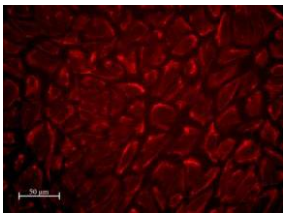

4 hrs OGD + Ro-32-0432

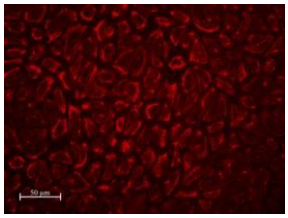

4 hrs OGD + R + Ro-32-0432

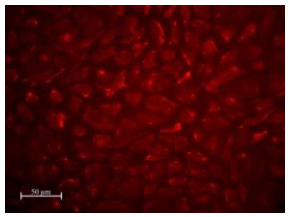

4 hrs OGD + NT siRNA

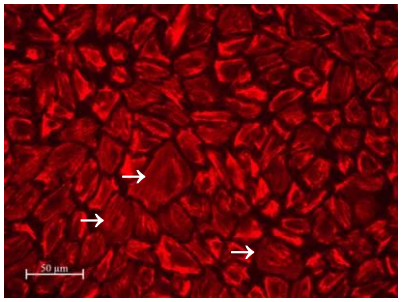

4 hrs OGD + R + NT siRNA

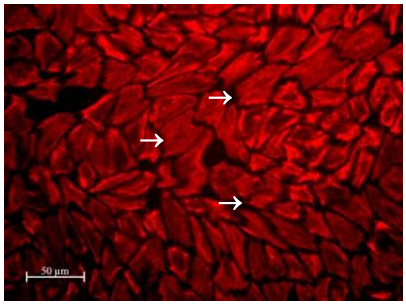

4 hrs OGD + PKC-α siRNA

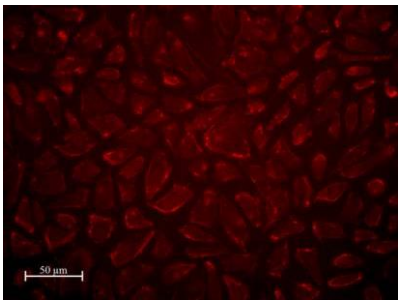

4 hrs OGD + R + PKC-α siRNA